JAERI-Conf
96-015

PROCEEDINGS OF THE 2nd MEETING ON TUNNELING REACTION AND LOW TEMPERATURE CHEMISTRY, 96 AUGUST

August 22~23, 1996, JAERI, Tokai, Japan

November 1996

(Eds.) Tetsuo MIYAZAKI* and Yasuyuki ARATONO

日本原子力研究所
Japan Atomic Energy Research Institute

本レポートは，日本原子力研究所が不定期に公刊している研究報告書です。
入手の問合わせは，日本原子力研究所研究情報部研究情報課（〒319-11 茨城県那珂郡東海村）あて，お申し越しください。なお，このほかに財団法人原子力弘済会資料センター（〒319-11 茨城県那珂郡東海村日本原子力研究所内）で複写による実費頒布をおこなっております。

This report is issued irregularly.
Inquiries about availability of the reports should be addressed to Research Information Division, Department of Intellectual Resources, Japan Atomic Energy Research Institute, Tokai-mura, Naka-gun, Ibaraki-ken 319-11, Japan.

編集兼発行　日本原子力研究所
印　　刷　㈱原子力資料サービス

JAERI−Conf 96−015

Proceedings of the 2nd Meeting on Tunneling Reaction and Low Temperature Chemistry — Tunneling Reaction and Biology —

August 22 - 23, 1996, JAERI, Tokai, Japan

(Eds. Tetsuo MIYAZAKI* and Yasuyuki ARATONO)

Advanced Science Research Center
Japan Atomic Energy Research Institute
Tokai-mura, Naka-gun, Ibaraki-ken

(Received October 14, 1996)

Present report is the proceedings of the 2nd Meeting on Tunneling Reaction and Low Temperature Chemistry held in August 22 to 23, 1996. The main subject of the meeting is "Tunneling Reaction and Biology".

The 1st meeting on "Tunneling Reaction and Low Temperature Chemistry -Tunneling Reaction and Cryotechnique-" was held in July 31 to August 1, 1995. During the past 1 year, the experimental research on the tunneling reaction of solid hydrogen isotopes at ultralow temperature progressed remarkably. The theoretical approach based on the multi-body reaction mechanism is going to start to explain the tunneling reaction in the solid phase as well as three-body treatment so far carried out.

Tunneling effect in living body proceeds at the temperature. About 80% of human body is composed of water. Thus, the vital functions in human body involve the transfer of atomic hydrogen or proton. As the tunneling phenomenon is caused by wave property of light particle, the biological reaction concerned with hydrogen atom or proton is expected to preferentially proceed through the tunneling process. From such a point of view, "2nd Meeting on Tunneling Reaction and Low Temperature Chemistry, -Tunneling Reaction and Biology-" was held. The number of the participants from various research fields such as medical science, pharmacy as well as physical chemistry was 40 and 12 invited lectures were presented.

---

* Nagoya University

The editors believe that the present proceedings will contribute to understanding of the tunneling reaction in biology and its related area.

Keywords: Tunneling Reaction, Biology, Vital Function,
Low Temperature Chemistry, Radiation Chemistry

JAERI－Conf 96－015

トンネル反応および低温化学についての研究会報告集（Ⅱ）
第２回低温化学セミナー「トンネル反応と生物効果」
1996年８月22日－８月23日、東海村

日本原子力研究所先端基礎研究センター
（編）宮崎　哲郎*・荒殿　保幸

（1996年10月14日受理）

本報告集は1996年８月22日から23日の２日間にわたって開催した第２回低温化学セミナーの講演のプロシーディングスである。今回の主題は「トンネル反応と生物効果」である。

第１回低温化学セミナー「トンネル反応と極低温技術」（JAERI-Conf 95-020）は1995年７月31日－８月１日に開催したが，この１年間で低温における水素同位体のトンネル反応に関しては，実験的研究が非常に進んだ。また理論的研究も従来の気相理論からのアプローチのみでなく固相の特質を最初から組み入れた理論計算がこれからなされようとしている。

生体内におけるトンネル効果は，生体温度で起るトンネル反応である。人体の約80％は水で占められており，従って生体内で起る生理機能の多くには水素原子あるいはプロトンが関与している。トンネル現象は原子の波動性に起因する現象である事から，波動性の最も強い水素原子の関与する生体内反応にはトンネル効果が寄与している可能性が高い。今回，そのような観点から，「トンネル反応と生物効果」についての研究会を開催した。研究会の参加者は，約40名で日頃交流の少ない理学，医学，薬学関係の研究者がそれぞれの立場から12件の講演を行った。

本報告集が生体系でのトンネル反応やその関連分野の研究の発展にいささかでも寄与できれば幸いである。

日本原子力研究所：〒319-11　茨城県那珂郡東海村白方白根2-4
＊名古屋大学

The 2nd Meeting on Tunneling Reaction and Low Temparature Chemistry, 96 August -Tunneling Reaction and Biology-

August 22-23, 1996

Japan Atomic Energy Research Institute
Tokai, Japan

Sponsored and Organized
by
Advanced Science Research Center,
Japan Atomic Energy Research Institute,
and
Japanese Society of Radiation Chemistry

Supported
by
Chemical Society of Japan
and
Japan Radiation Research Society

Contents

目　　次

1. Chemical Evolution in the Dust Grains in the Interstellar Medium

Kenzo Hiraoka
Faculty of Engineering, Yamanashi University

1. Introduction

In the diffuse interstellar clouds, ion-molecule reactions are the dominant processes for the formation of interstellar molecules. Because the temperature of the dense molecular clouds (i.e., dark clouds) is 10-20 K, all gases except for He, Ne and H_2 may be condensable on the surfaces of dust grains and form mantles on the dusts. In order to elucidate the chemical evolution in dark clouds, it is important to investigate the chemical processes taking place on the surfaces of dust grains and in their mantles.

The molecules such as NH_3, HCHO, CH_3OH, and hydrocarbons are most important for the evolution of life in the universe. However, the mechanisms for the formation of these molecules are known to be difficult to explain by the gas-phase ion-molecule reactions only. Although the solid-phase reactions on the cold dust grains are proposed for the formation of these molecules, there have been no attempts to give solid evidence for the occurrence of the reactions at low temperatures. In the present work, the experimental evidences for the importance of the chemical evolution taking place on the dust grains will be given[1-3].

2. Experimental

The schematic diagram of the experimental apparatus is shown in Fig.1. By using the bottle-neck quartz discharge tube 2, molecules or radicals are deposited on the surface of the cold head of the cryocooler at 13 K. The deposited sample was reacted

with hydrogen atoms which are generated by the plasm-activated H_2 gas using the bottle-neck discharge tube 1. The reaction products are analyzed by means of a temperature-programmed mass spectrometer. The energetic charged particles generated from the plasma-activated H_2 is completely eliminated by applying high voltage between the parallel electrodes(12) just outside the discharge tube 2.

3. Results and discussion

Figure 2 shows the temperature-programmed mass spectra of peaks with m/z=29, 30, 31, and 32 for H_2 plasma sprayed CO film at 13 K. The peaks appearing at about 110 K and 160 K correspond to the reaction products of formaldehyde and methanol, respectively. It is evident that CO film reacts with H atoms to form these molecules through the tunneling reactions. These results indicate that formaldehyde, which is the second most abundant molecule after H_2 in the interstellar medium is likely to be the mother molecule toproduce formaldehyde and methanol on the dust grains. It should be noted that the yields of products, CO→HCHO and HCHO→CH_3OH are 0.01 % and 50 %, respectively. That is, the former is very small but the latter is surprizingly large. It is evident that the reaction of H atoms with CO is slow whereas that with HCHO is much faster.

In the separate experiment, the reactions of H atoms with CH_3OH were investigated. To our surprise, CH_4 was detected as a major reaction product. This indicates the occurrence of the reaction,

$$CH_3OH + 2H = CH_4 + H_2O.$$

The present results suggest that the one of the most abundant molecule CO in the interstellar medium is the starting molecule for the formation of not only HCHO and CH_3OH but also H_2O and CH_4.

[1]K.Hiraoka et al.Chem.Phys.Lett.197(1992)292.
[2]K.Hiraoka et al.Chem.Phys.Lett.,229(1994)408.
[3]K.Hiraoka et al.Astrophys.J.443(1995)363.

Fig.1

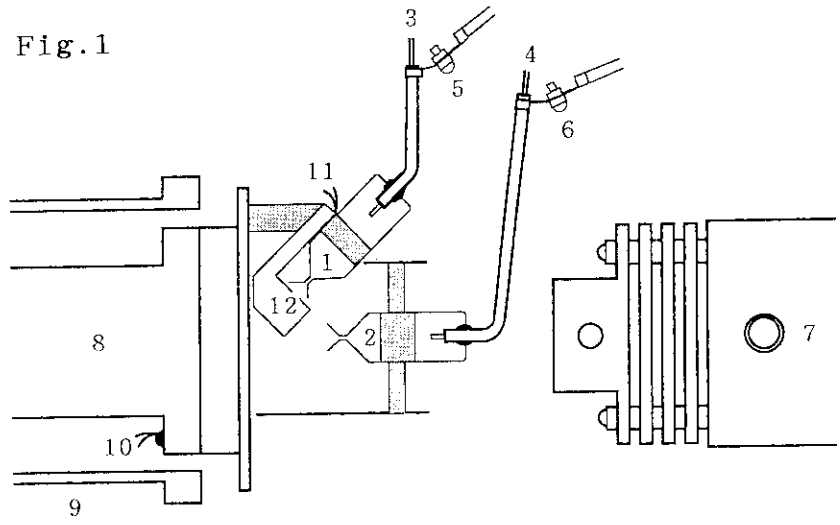

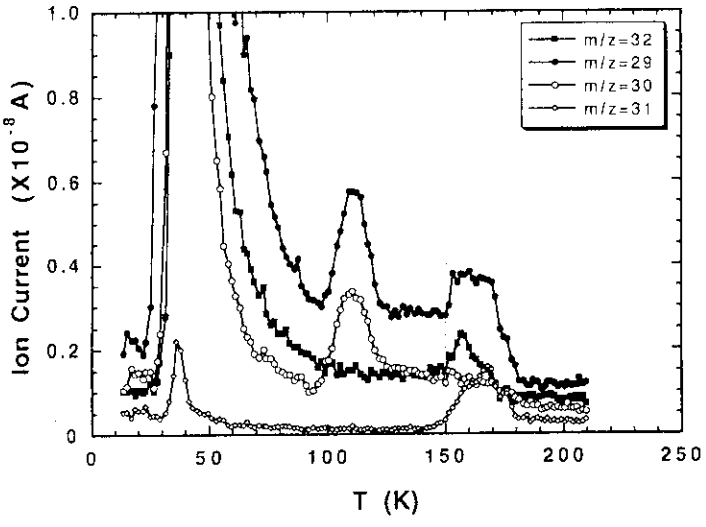

Fig. 2. Temperature-programmed mass spectra of peaks with $m/z=29$, 30, 31, and 32 for H_2 plasma sprayed CO film. The procedure of ((1) deposition of 10 monolayer thick CO, and (2) H_2 plasma spray over the deposited CO film for 5 min) was repeated 100 times and the temperature-programmed mass spectra for the multilayer sample were measured. The temperature of the cold head was kept constant at 13 K during the H_2 plasma spray over the deposited CO. The large peak at ≈ 35 K with $m/z=32$ is due to the desorption of O_2 which is contained in the vacuum chamber as a residual gas.

2. Time Evolution of Rate Constant for Tunneling Reaction $H_2 + D \rightarrow H + HD$ in Solid D_2–H_2 Mixtures at Very Low Temperature

Takayuki Kumada [a, *], Yasuyuki Aratono [a], Tetsuo Miyazaki [a, b]

[a] Advanced Science Research Center, Japan Atomic Energy Research Institute, Tokai-mura, Naka-gun, Ibaraki 319-11, Japan

[b] Department of Applied Chemistry, School of Engineering, Nagoya University, Furo-cho, Chikusa-ku, Nagoya 464-01, Japan

Abstract

Time dependence of the amounts of H and D atoms, produced by γ-radiolysis of D_2-H_2 (1 mol %) mixture, was measured upon the storage of the sample at 4.5 K by ESR spectroscopy. The amount of D atoms gradually decreases up to 190 minutes, while that of H atoms increase in ten minutes and then become a plateau value. The results were interpreted in terms of competition of a tunneling reaction $H_2 + D \rightarrow H + HD$ with combination reactions of D and H atoms. The results cannot be explained by a single value of a rate constant for the tunneling reaction used in homogeneous kinetics, but by time evolution of a rate constant.

1. Introduction

Chemical reactions in solid hydrogen have the following interesting properties. Because of small mass of hydrogen atom, large zero-point vibration and free rotation of a hydrogen molecule, the hydrogen atoms in solid hydrogen can be considered as quantum particles in quantum solid that is also of great interest in low-temperature physics. Hydrogen atoms react with neighboring H_2 (D_2) molecules at ultralow temperature near 4 K by a quantum tunneling without apparently forming the molecule H_3. The experiments at the ultralow temperature are appropriate for studying the tunneling reaction, since almost all thermally-activated processes are suppressed. Study of a quantum mechanical tunneling in a hydrogen atom - hydrogen molecule reaction has been important for elucidation of the theory of chemical kinetics, since it is a prototype of bimolecular reactions. Some kinds of chemical reactions in the solid phase cannot be expressed by homogeneous kinetics, but by dispersive kinetics [1]. Chemical kinetics in the solid hydrogen, which can be considered also as a prototype of solid kinetics, is also important for the elucidation of solid kinetics.

Miyazaki and his group have studied in detail the tunneling reaction of hydrogen

atoms in solid hydrogen [2 ,3]. In their data, the rate constant for $H_2 + D \rightarrow H + HD$ at 4.5 K is estimated as about 3.7×10^{-1} mol cm^{-3} s^{-1}. The rate constant for the tunneling reaction agrees qualitatively with that calculated for gas phase model [4, 5]. In their study, however, the rate constant was obtained from the data in the storage time within only 15 minutes [3]. Here we have measured the tunneling reaction $H_2 + D \rightarrow H + HD$ up to 190 minutes and found that the rate constant depends on the storage time.

2. Experimental section

The purity of H_2 and D_2 was more than 99.999 and 99.5 mol %, respectively. The mixture of D_2 - H_2 (1 mol %) was sealed in a fused quartz tube and solidified by rapid cooling of the sample tube from room temperature to 4.2 K. The sample of solid hydrogen is 3.0 cm in height and 0.2 cm in width. It was irradiated at 4.2 K with γ-rays from a ^{60}Co source to a total dose of about 1.5 kGy. The H and D atoms, produced by the radiolysis, were measured at 4.5 K by a JES-FE2XG ESR spectrometer. The amount of hydrogen atoms was obtained by double integration of signals with a digitizer-personal computer system. The errors of the amount were about 10 %. As shown in ref. 3, in this system at 4.2 K, the tunneling reaction proceeds too slowly to measure. Therefore the time dependence of the rate constant cannot be studied clearly. Then, we tried to heat the sample so as to increase a rate constant for the tunneling reaction. Consequently, the temperature of 4.5 K was obtained by heating the sample in the liquid helium with an IR lamp illumination. The temperature of the sample was measured by a thin Au-Chromel thermocouple (0.012 cm in diameter) inserted into solid hydrogen. When the IR illumination was cut off, the temperature of the sample was quickly cooled down to 4.2 K in several seconds.

3. Result

When the D_2 - H_2 (1 mol %) mixture is irradiated with γ-rays, D and H atoms are produced and they can be measured by ESR. Figure 1 shows the relative amounts of D atoms, depicted by open circles (○), and H atoms, depicted by closed squares (■) upon the storage of the irradiated mixture at 4.5 K. The amount of the D atoms decreases gradually, while that of H atoms increases rapidly especially in the initial 15 minutes and then are approximately constant after 15 min. ESR linewidths of D atoms, depicted by triangles, are almost constant during storage of the irradiated sample. The absolute concentrations of D (H) atoms were determined by G value (5.4) of D and H amount in the radiolysis of the D_2-H_2 (1 mol %) mixture at 4.2 K [6]. Ivliev et. al. have

also studied the amounts of D and H atoms in the D_2-H_2 mixtures at 5.2 K up to 170 minutes [7]. In their experiment, D and H atoms were produced with a rf discharge of D_2 and H_2 gas and condensed on a cold substrate located in a ESR cavity.

4. Discussion

4. 1. Rate constants for the tunneling reaction $H_2 + D \rightarrow H + HD$

All possible elementary reactions are represented as follows.

$$D_2\ (H_2) \rightsquigarrow D\ (H) \quad (1)$$
$$D + D \rightarrow D_2 \quad (2)$$
$$D + H \rightarrow DH \quad (3)$$
$$H + H \rightarrow H_2 \quad (4)$$
$$H_2 + D \rightarrow H + HD \quad (5)$$
$$D_2 + H \rightarrow D + HD \quad (6)$$

D atoms, produced by radiolysis (reaction 1), diffuse in solid deuterium and combine with other D atoms (reaction 2) or H atoms (reaction 3). Similarly H atoms combine with other atoms (reaction 3 and 4). If only these combination reactions take place at 4.5 K, both H and D atoms should decrease during the storage of the sample. The initial increase of the amount of H atoms indicates that H atoms can be produced by a tunneling reaction $H_2 + D \rightarrow H + HD$ (reaction 5). Since the reaction $D_2 + H \rightarrow HD + D$ is endothermic process, it cannot occur at the ultralow temperature.
Then the amounts of D and H atoms are expressed by the following two equations.

$$\frac{d[D]}{dt} = -2k_2[D]^2 - k_3[D][H] - k_T[D][H_2] \quad (7)$$

$$\frac{d[H]}{dt} = -2k_4[H]^2 - k_3[D][H] + k_T[D][H_2] \quad (8)$$

where k_2, k_3, k_4, and k_T are the rate constants for the reactions (2), (3), (4), and (5), respectively. Since H (D) atoms combine with other H (D) atoms without any activation energy, it is assumed here that they combine with other atoms in every encounter. The combination reaction can be regarded as a diffusion-controlled reaction. Then,

$$k_2 = 4\pi r(D_D + D_D) \quad (9)$$
$$k_3 = 4\pi r(D_D + D_H) \quad (10)$$
$$k_4 = 4\pi r(D_H + D_H) \quad (11)$$

where D_D and D_H are the diffusion coefficients of D and H atoms, respectively, and r is the contact distance between two atoms in the combination reaction. When k_D and k_H

are denoted here as $4\pi r D_D$ and $4\pi r D_H$, respectively, eqs. (7) and (8) are represented by

$$\frac{d[D]}{dt} = -4k_D[D]^2 - (k_D + k_H)[D][H] - k_T[D][H_2] \quad (12)$$

$$\frac{d[H]}{dt} = -4k_H[H]^2 - (k_D + k_H)[D][H] + k_T[D][H_2] \quad (13)$$

The initial concentrations of D atoms and H atoms at the beginning of the storage were determined by ESR measurement. If k_D, k_H, and k_T are given, time dependence of the amounts of D and H atoms can be calculated by integration of the two simultaneously differential equations (12) and (13) with a computer.

Figure 2 shows the relative experimental amounts of H atoms (depicted by ■) and D atoms (depicted by ○) in the D_2 - H_2 mixtures upon storage of the sample. The Figures [A], [C] and [E] in the left - hand side show the behavior of D and H atoms in the D_2-H_2 (1 mol %) mixture produced by γ-ray irradiation (cf. Fig. 1). The Figures [B], [D] and [F] in the right - hand side show that in D_2-H_2 (ca. 1 - 4 mol %) at 5.2 K produced by the rf. discharge (cf. quoted from ref. [7]). Solid and dashed lines are theoretical amounts of H and D atoms, respectively, calculated from the kinetic equations. The lines in [A] and [B] are typical theoretical ones fitted by use of three parameters k_H, k_D and k_T in eqs. (12) and (13). Though the absolute concentrations of H and D atoms are unknown in the case of ref. [7], the relative concentrations of them can be used in kinetic treatment for the fitting. Both theoretical lines in [A] and [B] cannot account for the experimental data in the whole timescale. Since the three parameters are chosen in order to fit the lines to the experimental amount in the range of the long storage time, the striking differences between the theoretical amount and experimental one are observed in the initial storage time. On the other hand, when the theoretical lines are fitted to the experimental amount in the initial storage of time, the large differences between the theoretical amount and experimental one appear in the long storage time. Therefore, it is concluded that the theoretical amount cannot coincide with the experimental ones, when one set of values is assumed for each three parameters k_D, k_H, and k_T. Since it has been reported that the rate constant for a chemical reaction in the solid phase depends upon time of the reaction [1], we will consider the following two models.

When solid hydrogen is produced by rapid cooling to 4 K, the solid consists of a mixture of two crystalline states of f.c.c. and h.c.p. [8, 9]. In order to analyze the

results simply, it is assumed here that the reactions in the solid hydrogen take place in two different regions, where rate parameters show different values. In the first model, two different values for the rate parameter for diffusion of H (or D) atoms, k_H (or k_D), were taken in the two regions, but the same rate constant for the tunneling reaction, k_T, was taken here. Figures [C] and [D] show typical theoretical amount based upon a model of two values for k_H and k_D and one value for k_T. As same as figures [A] and [B], the theoretical lines do not coincide with experimental amount. If the calculated lines are fitted to the experimental amount in the range of the long storage time, the striking differences between the theoretical amount and experimental one are observed in the initial storage time. Inversely when the fitting performed in the initial storage time, the experimental results in the long storage time cannot be explained by the theoretical model. In all cases, experimental amount cannot be explained by this model. This is because k_T is taken as a single value in the two regions. As shown in Fig. 1 the rapid increase of H atoms in the initial storage time suggests a rapid tunneling reaction, while the nearly constant value of the H atoms and the gradual decrease of the D atoms in the long storage time suggest the presence of a slow tunneling reaction.

In the second model, two different values for k_T were taken in the two regions, while the same value was assumed for k_H (or k_D) in the two regions. The typical theoretical lines in [E] and [F] coincide with the experimental amount in the whole range of the storage time. It is concluded that the rate constants for the tunneling reaction (5) consist of two different values, i.e., a fast rate constant and the slow one. Table 1 shows the two different rate constants, i.e., k_T (fast) and k_T (slow), for the tunneling reaction, which coincide with the experimental amount in various ratios (k_H / k_D) of the diffusion coefficient of H atoms to that of D atoms. Though the absolute concentrations of H and D atoms are unknown in the case of ref. [7], the relative concentrations of them can be used in kinetic treatment for the fitting, because the fitting parameters of k_T(fast) / k_T(slow) are independent of the initial absolute concentrations of H and D atoms. Only in the case of $0 < k_H < k_D$, the experimental results can be explained in the whole timescale. The k_H / k_D less than 0.01 does not revised the fitting (cf. Table 1). It indicates that D atoms diffuse faster than H atoms. It was suggested previously that the D atoms migrate faster than H atoms in solid D_2, when the diffusion is caused by the repetition of tunneling reactions [10]. Though the absolute ratio (k_T(fast) / k_T(slow)) cannot be determined from the present result, it can be concluded that the rate constant for the tunneling reaction consists at least of two values. Tunneling reactions in such a simple crystal as solid hydrogen cannot be explained by the homogeneous kinetics, but by inhomogeneous kinetics that assumes two rate constants.

Now we will discuss the causes of two kinds of rate constants.

4. 2. Plausible causes of two kinds of rate constants for tunneling reaction

4. 2. 1. Different reactivity between ortho and para hydrogen

Since n-H_2 consists of 75 % o-H_2 and 25 % p-H_2, one of the plausible causes is due to different reactivity between ortho and para hydrogen molecules with deuterium atoms. It was reported previously that the rate constant for the tunneling reaction p-H_2 + H (T) → H + H_2 (HT) is only by three times larger than that for the tunneling reaction o-H_2 + H (T) → H + H_2 (HT) [11]. Thus, the large difference between k_T (fast) and k_T (slow) cannot be ascribed to the different reactivity between ortho and para hydrogen.

4. 2. 2. Inhomogeneity of temperature in the D_2 matrix

The sample was immersed in liquid helium and irradiated with a IR lamp to increase temperature up to 4.5 K. So it is doubtful whether the temperature of the sample is uniform or not. The inhomogeneity of the temperature may cause different rate constants for the tunneling reaction.

Since a reliable potential energy curve for a reaction H_2 + D → H + HD can be obtained, the exact calculations for a tunneling reaction H_2 + D → H + HD have been done by two groups [4, 5]. According to their calculations, a remarkable temperature dependence of a rate constant appears only above 30 K. In fact, the ratio of the rate constant for the tunneling reaction at 10 K to that at 4 K, i.e., k_T (10 K) / k_T (4 K), is less than 2. Thus, a large difference in the rate constant for the tunneling reaction cannot be explained by the inhomogeneity of temperature. It is pointed out, however, that the calculation is based upon the model that a tunneling reaction takes place without any interactions with surrounding molecules. If the tunneling reaction in solid hydrogen is affected significantly by surrounding phonons, the small change in temperature may cause a large difference in the rate constant for the tunneling reaction.

4. 2. 3. Different reactivity of D atoms trapped in interstitial or substitutional sites

The structure of trapping sites of D atoms, such as interstitial and substitutional sites, in D_2 - H_2 (1 %) crystal is very important factor for the tunneling reaction of D atoms. The distances between a D atom and neighboring D_2 (H_2) molecules are 2.32, 2.68 and 3.79 Å for a tetrahedral interstitial site, an octahedral interstitial site and a

substitutional site, respectively [9]. It is expected that the large differences in the distance are related to the large difference in the rate constants, if D atoms are trapped in the different sites. But this possibility is denied by the data of ESR linewidth shown in Fig. 1. The ESR linewidth is caused by superhyperfine interactions of D atoms with surrounding hydrogen molecules, where the linewidth (Δ H) is roughly related to the distance (r) between D atoms and the neighboring hydrogen molecules by the following equation [12, 13].

$$\Delta H \propto r^{-3} \qquad (14)$$

Since the ESR linewidth of D atoms are almost constant within experimental errors (7 %) in a whole storage time, the distance between a D atom and surrounding H_2 molecule is kept to be constant within the fluctuation of 3 %, indicating that the trapping site of D atoms are the same during the tunneling reactions. Thus, the different rate constants for the tunneling reaction D + H_2 cannot be ascribed to the difference of trapping sites of D atoms, such as interstitial and substitutional sites.

5. Conclusion

It is summarized that tunneling reactions even in such the simplest crystal as solid hydrogen cannot be explained by a homogeneous kinetics, but by time-evolution of rate constant. A tunneling reaction $H_2 + D \rightarrow H + HD$ may take place in the solid hydrogen, followed by a displacement of surrounding hydrogen molecules [$(D_2)_n$], which is also caused by tunneling.

$$H_2 + D\,(D_2)_n \rightarrow H\,(D_2)_n + HD \qquad (15)$$

Thus, the rate constant for the tunneling reaction is probably affected significantly by a little change of environment, such as temperature and different crystalline structures. The further study of environmental effects on tunneling reactions in solid hydrogen that is one of the simplest crystal will reveal the essential factors in a tunneling reaction and solid kinetics.

Acknowledgment

We thank to Dr. Toshiyuki Takayanagi of Japan Atomic Energy Research Institute for his helpful discussions. This work is supported in part by a Grand-in-Aid for Scientific Research from the Japanese Ministry of Education, Science, and Culture.

References

[1] A. Plonka, Progress in Reaction Kinetics, 16 (1991) 157.

[2] T. Miyazaki, Radiat. Phys. Chem. 37 (1991) 635.

[3] T. Miyazaki, S. Kitamura, H. Morikita and K. Fueki, J. Phys. Chem. 96 (1992) 10331.

[4] T. Takayanagi, N. Masaki, K. Nakamura, M. Okamoto, S. Sato and G. C. Schatz, J. Chem. Phys. 86 (1987) 6133; T. Takayanagi and S. Sato, J. Chem. Phys. 92 (1990) 2862.

[5] A. C. Hancock, C. A. Mead, D. G. Truhlar and A. J. C. Valandas, J. Chem. Phys. 91 (1989) 3492.

[6] T. Miyazaki, M. Kato, and K. Fueki, Radiant. Phys. Chem. 36 (1990) 501.

[7] A. V. Ivliev, A. S. Iskovskikh, A. Ya. Katunin, I. I. Lukashevich, V. V. Sklyarevskiĭ, V. V. Suraev, V. V. Filippov, N. I. Filippov and V. A. Shevtsov, Pis'ma Zh. Eksp. Teor. Fiz. 38 No. 7 (1983) 317 [JETP Letters 38 (1983) 379].

[8] G. Collins, E. Mapoles, W. Unites and T. Bernat, Proceedings of Conference on the Physics and Chemistry of Quantum Solids, Fluids, Films and Clusters, California, U.S.A., Feb. 15, 1995.

[9] P. C. Souers, Hydrogen Properties for Fusion Energy (University of California Press, 1986).

[10] T. Miyazaki, K. Lee, K. Fueki and A. Takeuchi, J. Phys. Chem. 88 (1984) 4959.

[11] Y. Fujitani, T. Miyazaki, N. Masaki, Y. Aratono and E. Tachikawa, Chem. Phys. Letters. 214 (1993) 301.

[12] C. P. Slichter, Principles of Magnetic Resonance (Harper & Row, New York, 1963) ch 3.

[13] T. Miyazaki and H. Morikita, Bull. Chem. Soc. Jpn. 66 (1993) 2409.

Table 1. Two rate constants for tunneling reaction $H_2 + D \rightarrow H + HD$ in solid hydrogen

condition of calculation [a]	rate constant [b]		ratio [b]	ratio [c]
(k_H / k_D)	k_T(fast)	k_T(slow)	k_T(fast)/k_T(slow)	k_T(fast)/k_T(slow)
1	19	0.23	83	31
0.1	12	0.06	200	100
0.01	12	0.03	400	110
0	11	0.03	～400	100

[a] Rate constants were obtained by assuming the various ratios (k_H / k_D) of diffusion coefficients of H and D atoms (see text).

[b] The values were obtained from the results in this work. Rate constants are expressed in unit of cm^3 mol^{-1} s^{-1}

[c] The values were obtained from the results quoted from ref. [7].

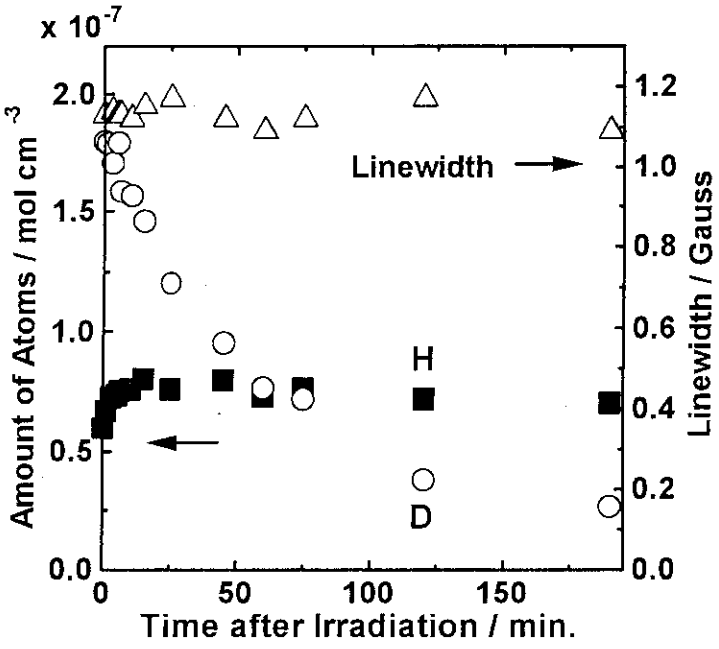

Fig. 1. Effect of storage of γ-irradiated D_2-H_2 (1 mol %) at 4.5 K. The initial concentrations of D and H atoms are 1.8 × 10^{-7} and 6.0 × 10^{-8} mol cm^{-3}, respectively. (○) D atoms, (■) H atoms, (△) ESR linewidth of D atoms represented in gauss.

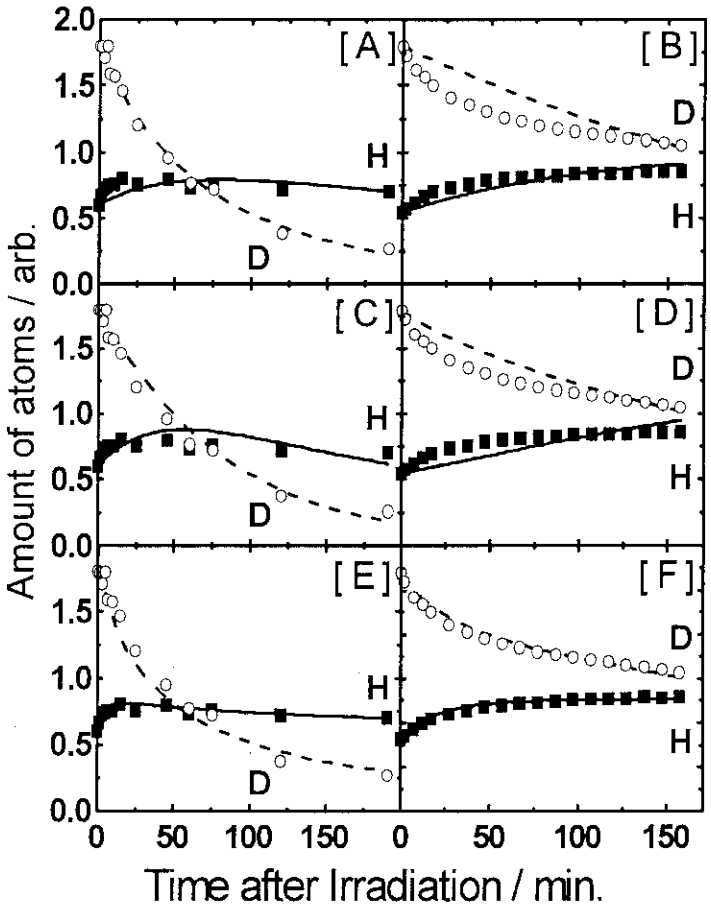

Fig. 2. Effect of storage of γ-irradiated D_2 - H_2. Results in the left - hand side are D_2 - H_2 (1 mol %) at 4.5 K obtained in this work. Those in the right - hand side are D_2 - H_2 (1 - 4 mol %) at 5.2 K quoted from ref. [7]. (○) experimental amount of D atoms, (■) experimental amount of H atoms, (- - -) simulated amount of D atoms, (——) simulated amount of H atoms. The simulations in [A] and [B] are based upon a model of a single value of diffusion coefficient and a single value of rate constant for a tunneling reaction. Those in [C] and [D] are based upon a model of two values of diffusion coefficients and a single value of a rate constant for reaction. Those in [E] and [F] are based upon a model of one value of diffusion coefficient and two values of a rate constant for a tunneling reaction (see text).

3. Temperature Dependence of Rate Constant for Tunneling Reaction HD + D → H +D_2 in Low Temperature Region 2.6–6.5 K: Experimental Evidence of Phonon–Assisted Tunneling

Takayuki KUMADA[a], Kenji KOMAGUCHI[a], Yasuyuki ARATONO[a], and Tetsuo MIYAZAKI[a,b]

[a] *Advanced Science Research Center, Japan Atomic Energy Research Institute, Tokai-mura, Naka-gun, Ibaraki 319-11, Japan.*

[b] *Department of Applied Chemistry, School of Engineering, Nagoya University, Furo-cho, Chikusa-ku, Nagoya 464-01, Japan.*

Abstract

Rate constants for the tunneling reaction, HD + D → H + D_2, in solid HD have been determined by using ESR in the very low temperature range of 2.6 K - 6.5 K. The rate constants increase steeply with increasing temperature above 5 K, while they are almost independent of temperature below 5 K. The results above 5 K do not coincide with theoretical values calculated by the gas phase model. Phonon-assisted mechanism is proposed to account for the remarkable temperature dependence of the tunneling reaction in solid HD.

Introduction

Tunneling reactions have been subjected to experimental and theoretical studies, because of fundamental importance not only in chemical kinetics at low temperatures but also in solid state physics and biological reactions. Miyazaki *et al.* have studied the hydrogen atom-hydrogen molecule reactions such as HD + D → H + D_2 in solid hydrogen [1, 2, 3]. That the quantum tunneling effect dominated the reaction in very low temperature is strongly indicated by the following two reasons. First, the absolute rate constant of the reaction has been estimated experimentally as 3.5 x 10^{-27} $cm^3molecule^{-1}s^{-1}$ at 4.2 K. The rate constant is much higher than that (*ca.* 10^{-400} $cm^3molecule^{-1}s^{-1}$) for the thermally-activated reaction, if the reaction would take place at 4.2 K by passing over a potential energy barrier (6.2 x 10^{-20} J $molecule^{-1}$) for the reaction [4]. Second, the significant isotope effect on the rate constant has been observed for reactions (1) and (2) at 4.2 K. The ratio of the rate constants, k_1/k_2, was

more than 3 x 10^4 [3].

$$H_2 + D \xrightarrow{k_1} H + HD \quad \cdots\cdots (1)$$

$$D_2 + H \xrightarrow{k_2} D + HD \quad \cdots\cdots (2)$$

On the other hand dynamical calculations for the hydrogen atom-hydrogen molecule tunneling reactions have been studied independently by two groups, Takayanagi *et al.* [4, 5] and Hancock *et al.* [6]. Regardless of the potential surfaces used, the calculations have shown that the rate constants are almost constant below 50 K and increase with increasing temperature above this temperature.

Recently, Kumada *et al.* have found that the tunneling reaction $H_2 + D \rightarrow H + HD$ has two distinct rate constants in solid D_2-H_2 mixture at 4.5 K [7]. The magnitude of the relative ratio of the two rate constants has been estimated to be more than 100. They have suggested that a slight inhomogeneity of temperature in the sample causes the large difference in the observed rate constants for the reaction.

The temperature dependence of the rate constants for the tunneling reactions of hydrogen atom-hydrogen molecule systems has never been studied. Here, we have found that the rate constants for the tunneling reaction $HD + D \rightarrow H + D_2$ strongly depend on temperature above 5 K. The results cannot be explained with any theoretical calculation based upon the gas phase model.

Experimental

The hydrogen deuteride (HD) was purchased from Isotec. Inc. The HD gas is 96.7 % purity, which contains H_2 (1.8 mol %) and D_2 (1.5 mol %) as contaminants. The HD gas (1.0 x 10^{-2} mol) was introduced into a Pyrex vessel (volume: *ca.* 260 cm^3) connecting with a quartz tube (diameter: 0.5 cm, length: 20 cm) for ESR measurements. The samples were prepared on a vacuum line. H and D atoms were produced in solid HD irradiated by white x-ray (Cu; 50 kV-40 mA) at 4.2 K for 2 hr in the ESR cavity. Then, the sample temperature was altered to the selected temperature before measurements of H and D atoms were begun. The temperatures were exactly controlled by a Model 9650 Cryogenic Temperature Indicator/Controller (Scientific Instruments, Inc.) combined with a cryostat using liquid helium as a coolant within an error of ±0.02 K. After the sample being at the corresponding temperature, the ESR spectra of H and D atoms were recorded on JEOL JES-TE200 spectrometer at a microwave power level of 2 nW, at which microwave power-saturation of the signals does not occur. The yields of signals, [H] and [D], were obtained by use of HP 9000 Model 382 workstation connected to the spectrometer.

Results and Discussions

Time-courses of D and H atoms in solid HD at 3.5 K and 5.8 K are shown in Figure 1 and Figure 2, respectively. The amounts of D and H atoms are shown by open and closed circles, respectively. The initial amounts of D atoms are considerably smaller than those of the H atoms just after x-ray radiolysis. A certain amount of D atoms already reacted with HD molecules during the irradiation.

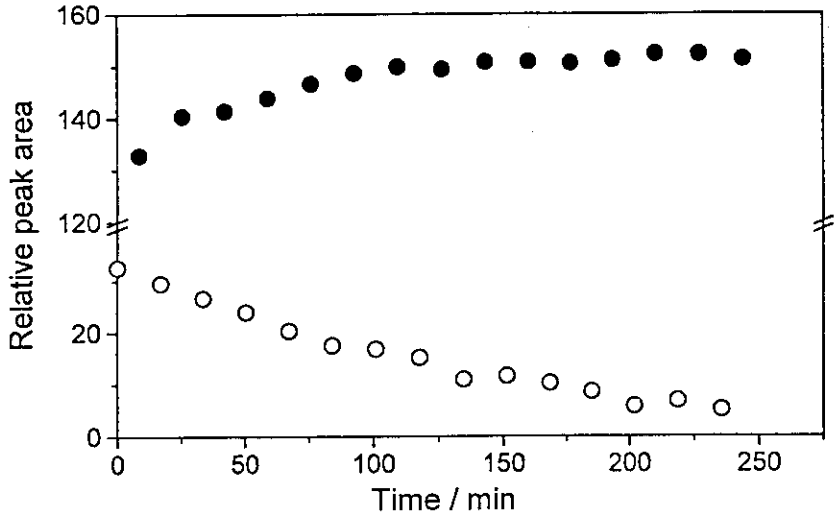

Figure 1. Time-course of relative yields of H (●) and D (○) atoms in solid HD at 3.5 K immediately after the x-ray radiolysis of HD at 4.2 K.

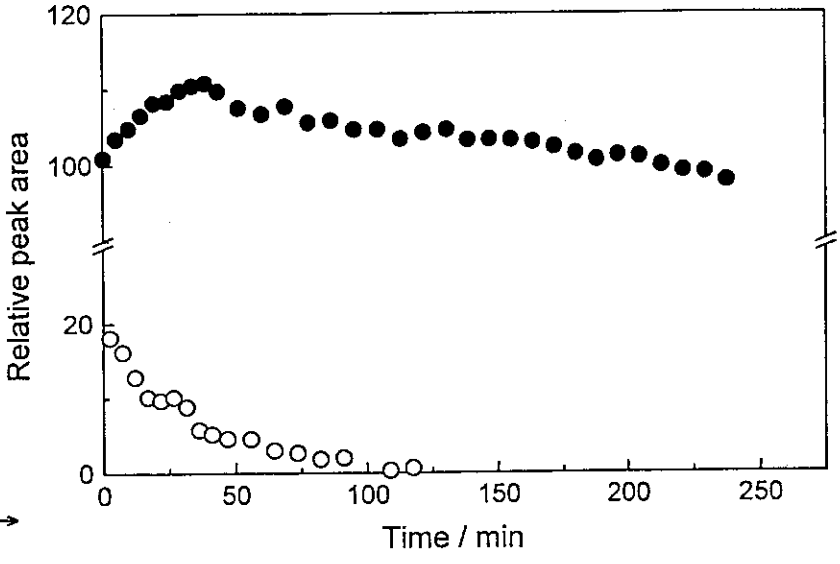

Figure 2. Time-course of relative yields of H (●) and D (○) atoms in solid HD at 5.8 K. The H and D atoms were produced by x-ray radiolysis of HD at 4.2 K.

The D atoms decay with the tunneling reaction HD + D → H + D_2, not by the recombination reaction upon storage below 6.5 K. The tunneling reaction should predominately proceed over the recombination D + D → D_2 which is followed by migration of D atoms to encounter each other in solid HD. This expectation is supported by the concomitant increases in H atoms as shown in Figures 1 and 2. After the D atoms have decayed, the recombination reaction of H atoms, H + H → H_2, occurring very slowly can be observed at 5.8 K. On the other hand, above 7 K the recombination reaction takes place faster than the tunneling reaction HD + D → H + D_2. The analysis considering all side reactions H + H → H_2, D + D → D_2, and H + D → HD gave the rate constant of 24 x 10^{-27} cm^3 $molecule^{-1}$ s^{-1} for the tunneling

reaction at 5.8 K, which is almost identical to 21 x 10^{-27} cm^3 $molecule^{-1}$ s^{-1} obtained by the simplified analysis where those side reactions were ignored. Therefore, the recombination reactions are negligible in the low temperature region. Incidentally the reaction HD + H → D + H_2 can be ruled out in the low temperature region because of its endothermic process. Thus, the main reaction scheme can be represented by reactions (3) and (4).

$$HD \xrightarrow{x-ray} H + D \qquad \text{----------(3)}$$

$$HD + D \xrightarrow{k_t} H + D_2 \qquad \text{----------(4)}$$

$$-\frac{d[D]}{dt} = k_t[HD][D] \qquad \text{----------(5)}$$

$$k_t[HD]=k' \qquad \text{----------(6)}$$

On the assumption that the reaction is regarded as a quasi-first-order reaction as shown in equation (6) because of a large excess amount of HD (5 x 10^{-2} mol cm^{-3}) in the reaction system. Then, the absolute rate constant, k_t, was determined at each temperature.

Figure 3 shows the plots of ln k_t *vs.* 1/T. The present results, summarised in Table 1, are depicted by closed circles. Additionally theoretical values obtained by use of different potential energy surfaces for the reaction are shown by four lines, where the values at 4.2 K are fitted to the experimental values at 4.2 K [4, 5, 6]. The present experimental rate constant at 4.2 K, obtained by x-ray irradiation, is 3.8 x 10^{-27} cm^3 $molecule^{-1}$ s^{-1}, which coincide well with those (*ca.* 3.5 x 10^{-27} cm^3 $molecule^{-1}$ s^{-1}, depicted by triangles) obtained by x-ray irradiation

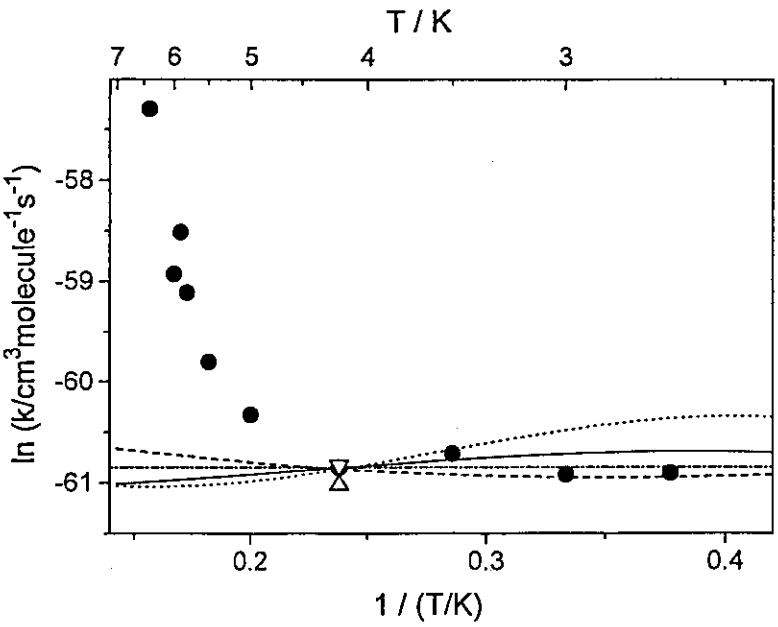

Figure 3. Plots of ln k vs. 1/T. The rate constants k (●) were experimentally determined for the tunneling reaction, HD + D → H + D_2, in solid HD. – – – –, –·–·–·–, and ····· lines indicate the theoretical calculations for the reaction based upon LSTH potential surface, DMBE with Van der Waals well, and LSTH with Van der Waals well potential surfaces, respectively [4, 5]. ——— is based upon SCSA method [6]. (△) and (▽) are experimental values reported previously [3].

[2, 3].

The observed rate constants, however, deviate from the calculated ones above 5 K (Figure 3). It is impossible to explain the drastic increase of the rate constants with any gas phase model. The theoretical calculations are probably not so helpful in discussing the solid phase reactions above 5 K.

Table 1. Rate constants k_t of the tunneling reaction HD + D → H + D_2 in the temperature range 2.65 K-6.4 K[a].

Temperature / K	2.65	3.0	3.5	4.2	5.0	5.5	5.8	5.9	6.0	6.4
k_t x 10^{-27}/cm^{3}molecule^{-1}s^{-1}	3.6	3.5	4.3	3.8	6.3	11	21	39	26	130

a: within an error ± 5 %

In the previous theoretical studies on the hydrogen atom-hydrogen molecule reactions caused by a tunneling effect, the temperature dependencies of the rate constants are essentially determined by
the Boltzmann distribution of the reaction system. Therefore, the rate constants increase with a increase of temperature above 50 K, while they are almost independent of temperature below 50 K, despite of improvements of the potential surface employed.

The remarkable temperature dependence of the rate constant for the tunneling reaction observed above 5 K needs a new theoretical model. As an environmental effect in solid, a phonon effect and discrete energy levels of the reaction systems should be taken into account. The number of the reaction systems in the higher levels increase with only a slight increase in temperature. The higher states excited by phonon led to the increase of the probability to match the initial and final states, resulting in the acceleration of the tunneling probability above 5 K.

The activation energy, E_a, was evaluated to be 95 K (1.3 x 10^{-21} J molecule^{-1}) from the slope in the temperature region between 5.4 K and 6.5 K in Figure 3. It is point out that the activation energy (95 K) is approximately the same order of magnitude as the Debye temperature (110 K) of solid HD [8].

In conclusion, the phonon-assisted mechanism is suggested for the tunneling reaction in solid HD at low temperatures. The chemical kinetics in solid phase can not be discussed no longer without taking the solid effect into account in a typical quantum matrix of solid hydrogen. Further theoretical calculations with a new model applicable to solid phase are required to clarify the tunneling reactions at very low temperatures.

Acknowledgment

The authors wish to thank Dr. T. Takayanagi of Japan Atomic Research Institute for many valuable discussions. This research was supported in part by a Grand-in-Aid for Scientific Research from the Japanese Ministry of Education, Science, and Culture.

References

[1] T. Miyazaki, K-P. Lee, K. Fueki and A. Takeuchi, *J. Phys. Chem.* **88** (1984) 4959.

[2] T. Miyazaki, N. Iwata, K-P. Lee and K. Fueki, *J. Phys. Chem.* **93** (1989) 3352.

[3] T. Miyazaki, *Radiat. Phys. Chem.* **37** (1991) 635.

[4] T. Takayanagi, N. Masaki, K. Nakamura, M. Okamoto and G. C. Schatz, *J. Chem. Phys.* **86** (1987) 6133.

[5] T. Takayanagi and S. Sato, *J. Chem. Phys.* **92** (1990) 2862.

[6] G. C. Hancock, C. A. Mead, D. G. Truhlar and A. J. C. Varandas, *J. Chem. Phys.* **91** (1989) 3492.

[7] T. Kumada, Y. Aratono and T. Miyazaki, *Chem. Phys.* (1996), in press.

[8] I. F. Silvera, *Rev. Mod. Phys.* **52** (1980) 393.

4. Decay Behaviors of H_2^- Anions in Solid Parahydrogen :Effect of Nuclear Spins on Chemical Reactions

Takayuki Kumada,[†*] Hirohisa Inagaki,[‡] Naoki Kitagawa,[‡]
Kenji Komaguchi,[†] Yasuyuki Aratono,[†] Tetsuo Miyazaki[†‡]

[†]Advanced Science Research Center, Japan Atomic Energy Research Institute,
Tokai-mura, Naka-gun, Ibaraki 319-11, Japan
[‡]Department of Applied Chemistry, School of Engineering,
Nagoya University, Furo-cho, Chikusa-ku, Nagoya 464-01, Japan

Decay processes of H_2^- anions in γ-rays-irradiated solid parahydrogen were studied by using ESR spectrometer. The following interesting results were obtained. First, the initial amount of ortho-H_2^- anions in the γ-irradiated solid parahydrogen was three times as large as those of para-H_2^- anions. Second, the amount of para-H_2^- anions decreases faster than that of ortho-H_2^- anions upon storage of the irradiated samples at 4.2 K. Third, the decay rate of H_2^- anions is accelerated by the addition of D_2 molecules. Forth, H_2^- anions at 2.2 K decay faster than at 4.2 K. According to the parity conservation rule in a homonuclear diatomic molecule, the energy of ortho-H_2^- anions at the ground state is lower than that of para-H_2^- anions, whereas that of ortho-H_2 molecules is higher than that of para-H_2 molecules at low temperatures. The first and second results are ascribed to para→ortho conversion of H_2^- anions. The third result indicates a transformation of H_2^- anion into $H_2 + e^-$ or $H + H^-$ caused by a distortion of the crystal around D_2 or HD molecules. The forth result suggests a coherent tunneling mechanism of diffusions of H_2^- anions in the solid parahydrogen.

Introduction

Solid hydrogen is a matrix of great interest that shows remarkable quantum phenomena.[1,2] Recently, Miyazaki has proposed that solid parahydrogen (p-H_2) , which has no nuclear spin moment, is a very useful matrix for a high resolution ESR spectroscopy at ultralow temperatures, at which unstable species are trapped. Because of absence of their superhyperfine interactions, the spectra narrow drastically.[3] In the γ-rays-irradiated solid p-H_2, we have found the new stable species of H_2^- anions for the first time, which are unstable in gas phase.[4] In addition, the new observation gives additional

interesting result. para-H_2^-(p-H_2^-) and ortho-H_2^-(o-H_2^-) are formed in the ratio of 1:3,[4] though the purity of p-H_2 molecules in the solid is higher than 95 %. It suggests that para→ortho conversion has occurred during the irradiation, while, in the case of H_2 molecule, ortho→para conversion generally occurs at low temperatures. If the para→ortho conversion of H_2^- anions still occurs after the irradiation, it should be detectable. In this study, we have examined the time evolution of the storage of para- and ortho-H_2^- anions in the γ-irradiated solid p-H_2 at 2.2 K and at 4.2 K. Effects of D_2 on the decay processes of H_2^- anions were also studied.

Experimental

p-H_2 samples were synthesized by normal hydrogen liquid passing through a column of iron hydroxide (III) (FeO(OH)) at 14 K. Purity of p-H_2 was more than 95 mol %. The samples solidified were irradiated at 4.2 K with γ-rays from a Co-60 source to a total dose of 0.3 kGy. In order to reduce the amount of color centers in γ-irradiated quartz, we have used a new cryostat for γ-irradiation. In some cases, the samples were irradiated with X-rays (60 kV, 45 mA) at 4.5 K. The radical species produced were measured by ESR spectroscopy at 4.2 K and at 2.2 K. The 2.2 K was produced by evacuating the liquid helium by a rotary pump. The relative amount of H_2^- anions was obtained by measuring the peak heights of the ESR spectra. It was verified that the influence of the color centers on the peak height is almost negligible, because the signals originated from color centers did not decay at all during the measurements. The details of the experimental procedure were described in the pervious paper.[5]

Results

Figure 1 shows the ESR spectrum of the solid parahydrogen γ-rays-irradiated at 4.2 K. The peaks, indicated by B1, B2, B3 and B4, are of H_2^- anions, while the peak indicated by A is due to other species that has not been identified yet. B1, B2, B3 and B4 peaks are attributed to the states of $|I=1, I_z=0\rangle$, $|0, 0\rangle$, $|1, 1\rangle$ and $|1, -1\rangle$ of H_2^-, where I and I_z indicate the spin quantum number and the spin magnetic quantum number, respectively.[4] So the B2 peak is of p-H_2^- and the others, B1, B3 and B4, are of o-H_2^-. As discussed above, it is interesting that the amount of o-H_2^- is by three times larger than those of p-H_2^-, while the concentration of p-H_2 in the solid is more than 95 %. When ortho-H_2 molecules (o-H_2) at 6 mol % were added to the solid p-H_2, the ratio of the amount of o-

H_2^- to that of p-H_2^- was not changed.

Figure 2 shows time-course of the intensities of H_2^- anions upon storage of γ-irradiated solid p-H_2 at 4.2 K. The intensities of B1 (I_{B1}) and B2 (I_{B2}) peaks in Figure 1, corresponding to the amounts of o-H_2^- and p-H_2^-, are represented by (●, ■, ▲) and (○, □, △), respectively. The experiments have been done for three different samples, depicted by circles, squares and triangles, respectively. As shown in the figure, the reproducibility of these data are good. The intensities of B3 peak (I_{B3}) and B4 peak (I_{B4}) could not be measured because of their poor S/N ratio. But their time-course is expected to be the same as that of B1, since they are attributed to ortho-H_2^- and just separated by their spin magnetic quantum number (I_z), which are not degenerated.[4]

Figure 3 shows the ratios of the amounts of p-H_2^- (○, □, △) and o-H_2^- (●, ■, ▲) to the total amount of H_2^- anions that are obtained from Figure 2 as $I_{B2}/(3\times I_{B1} + I_{B2})$ and $3\times I_{B1}/(3\times I_{B1} + I_{B2})$, respectively. Note that their denominators indicate the total amount of H_2^- anions ($I_{H_2^-}$) calculated as

$$I_{H_2^-} = I_{p\text{-}H_2^-} + I_{o\text{-}H_2^-} = I_{B1} + I_{B2} + I_{B3} + I_{B4} = 3 \times I_{B1} + I_{B2} \qquad (1)$$

The intensities of o-H_2^- increases upon the storage, while that of p-H_2^- decreases.

Figure 4 shows the initial intensities of B1 (▲) and B2 (▽) peaks in Figure 1, corresponding to amounts of o-H_2^- and p-H_2^-, respectively, in γ-irradiated p-H_2-D_2 mixtures as a function of concentrations of D_2 molecules at 4.2 K. The initial amount of H_2^- anions decreases as the concentration of D_2 in the solid increases.

Figure 5 shows time course of relative amounts of o-H_2^-(●, ■, ▲) and p-H_2^-(○, □, △) in γ-irradiated p-H_2 -D_2 mixtures upon the storage of the sample at 4.2 K, where all the amounts at t = 0 are normalized to 10. The amounts of the anions in the solids containing D_2 + HD at 0.03, 0.04 and 0.13 mol % are depicted by ● (○), ■ (□) and ▲ (△), respectively. It is pointed out that, in Figure 4 and 5, in any sample, a concentration of HD is 0.03 mol % which is obtained from natural abundance of D (0.015 mol %) in H.

Figure 6 shows time-course of the total amount of H_2^- anions ($I_{n\text{-}H_2^-}$) at 4.2 K (●, ■, ▲) and 2.2 K (◇, ▽). The experiments were done for three samples at 4.2 K and two ones at 2.2 K. It is interesting that H_2^- anions at 2.2 K apparently decay faster than at 4.2 K.

Discussion

Conversion of p-H_2^- Anions to o-H_2^- Anions. We now consider the problems why p-H_2^- anions decay faster than o-H_2^- and why the initial amount of o-H_2^- anions is higher than those of p-H_2^- anions. In a homonuclear diatomic molecule, its quantum state is restricted by its parity on exchanging each proton in a molecule. Since proton is a fermion, the total parity of the wave function of H_2^- molecule ($\Psi_{molecule}$) should be antisymmetric. Besides, it is represented as a product of that of each quantum state (φ), which is written as $\Psi_{molecule} = \varphi_{vibration} \times \varphi_{rotation} \times \varphi_{electron} \times \varphi_{nuclear\ spin}$.[6] Parities of wave functions on exchanging each proton in a H_2 molecule and a H_2^- anion are summarized in Table 1. Since a rotational wave function of a p-H_2 molecule is symmetric and that of an o-H_2 molecule is antisymmetric, p-H_2 and o-H_2 are in J=0 and J=1 rotational states at low temperatures, respectively. So the energy level of o-H_2 molecule at the ground state is 170.5 K higher than that of p-H_2. Accordingly, o-H_2 molecules convert into p-H_2 molecules by themselves, when magnetic perturbations exist around them. On the contrary, the electronic state of electrons in a H_2^- anion is $^2\Sigma^+_u$, which means antisymmetric on the exchanging, while that in H_2 molecule is $^1\Sigma^+_g$, which means symmetric.[7,8] Then, p-H_2^- and o-H_2^- anions at ground states are in J=1 and J=0 rotational states, respectively. Therefore, the energy of o-H_2^- anion becomes lower than that of p-H_2^- at 4 K. Accordingly, the result in Figure 3 is explained as para→ortho conversion of H_2^- anion under the magnetic perturbation caused by an unpaired electron in it.

$$\text{p-}H_2^- \rightarrow \text{o-}H_2^- \qquad (2)$$

When o-H_2 at 6 mol % was added to p-H_2, the ratio of the initial amount of o-H_2^- to that of p-H_2^- in the irradiated solid is the same as that in the irradiated pure p-H_2. Thus, the higher amount of o-H_2^- anions compared to that of p-H_2^- cannot be ascribed to the electron transfer from p-H_2^- anion to o-H_2 molecule (reaction 5).

$$\text{p-}H_2 \wedge\!\!\vee\!\!\vee\!\!\rightarrow \text{p-}H_2^+ + e^- \qquad (3)$$

$$e^- + \text{p-}H_2 \rightarrow \text{p-}H_2^- \qquad (4)$$

$$\text{p-}H_2^- + \text{o-}H_2 \rightarrow \text{p-}H_2 + \text{o-}H_2^- \qquad (5)$$

The high initial amount of o-H_2^- is probably due to the para→ortho conversion of p-H_2^-

during γ-irradiation (reaction 2). In contrast with the case of H_2 molecules, p-H_2^- anions convert into o-H_2^-.

Decay Mechanism of H_2^- Anions. H_2^- anions would migrate in the solid and finally meet to react with other species in the solid. Now, we will discuss the mechanism of the decay of H_2^- anions. Table 2 shows decay rates of H_2^- anions and initial amounts of H atoms and H_2^- anions at 4.5 K in the solid parahydrogen irradiated by X-rays at 17 min. and 150 min. Nevertheless of the large difference in their irradiation times, both decay rates are the same within their experimental errors, while the amounts of H_2^- anions and H atoms increase linearly with an increase of the irradiation time. As accompanied by the amount of H_2^- anions, that of cations is also expected to increase with an increase of the irradiation time for conservation of their charge in the solid. If H_2^- anions react with H atoms by the electron transfer reaction, $H_2^- + H \rightarrow H_2 + H^-$, or neutralize with cations, the decay rate H_2^- anions must be proportional to the amounts of H atoms or cations, respectively. However, as discussed above, it does not depend upon the amounts of H atoms or cations, suggesting that the disappearance process of H_2^- anions is due to neither the reaction with H atoms nor that with cations.

Now, the effect of the addition of D_2 on the decay of H_2^- anions will be discussed. Figure 4 shows that the initial intensities of B1(o-H_2^-) and B2(p-H_2^-) peaks in Figure 1 decrease as the concentration of D_2 in the solid increases. In addition to this, Figure 5 shows that the decay rates of both o-H_2^- and p-H_2^- anions are accelerated by addition of D_2 molecules, indicating that the H_2^- anions are broken by D_2 molecules in the solid. When H_2^- anions (probably electrons in H_2^-) migrate in the solid (reaction 6) and approach D_2 or HD molecules, they would be caught by distortions nearby D_2 or HD molecules in the solid and may be transformed into $H_2 + e^-$ or $H + H^-$ (reaction 7), which are not detectable by ESR.

$$H_2^- + H_2 \rightarrow H_2 + H_2^- \quad (6)$$

$$H_2^- \rightarrow H_2 + e \text{ or } H + H^- \quad (7)$$

The H_2^- anions in the solid are "crystal field induced H_2^-", so to speak. In gas phase, they are unstable and easily split into H_2 and e^-. Therefore, the H_2^- must sensitively depend on the crystal field around them. Note that electron transfer reaction $H_2^- + D_2 \rightarrow H_2 + D_2^-$ never happen in such a low temperature because of endothermic process. Experimentally, the ESR spectrum of D_2^- anions could not be detected neither.

Temperature Dependence of the Decay of H_2^- Anions Figure 6 shows that the H_2^- anions at 2.2 K decay faster than those at 4.2 K. Though the decay rate should decrease with decreasing temperature in the classical theory, it increases at lower temperature in this work. The decay rate is probably controlled by the rate for the diffusion of electron in H_2^- anions (reaction 6). Therefore, the data suggest that the electron in H_2^- anions migrate faster at the lower temperatures. It is probable that the reaction occurs via tunneling because of light mass of an electron. Moreover, its inverse temperature dependence of the diffusion rate is probably caused by repetition of coherent tunneling: particle-transfer without phonon absorption or emission.[9] For example, Kiefl et. al. previously reported that muon, whose mass is about 1/9 of a proton, migrates in ionic solids by coherent tunneling processes at ultralow temperatures.[10, 11] The rate for the diffusion increases clearly with decreasing temperature. By the same behavior as this, the temperature dependence on the decay of H_2^- anions shown in Figure 6 suggests that H_2^- anions diffuse in the solid parahydrogen by coherent tunneling.

Acknowledgment. The authors thank Emeritus Professor F. Nakano of Nagoya University and Doctor K. Yokoyama of Japan Atomic Energy Research Institute for their helpful comments and Mr. T. Nagasawa of Nagoya University for his help in the experiment. This work was supported in part by a Grant-in-Aid for Scientific Research from the Japanese Ministry of Education, Science and Culture.

References

(1) Kranendonk, V. *Solid Hydrogen*; Plenum: New York, 1983; Chapter 2.

(2) Sourers, P. C. *Hydrogen Properties for Fusion Energy* ; University of California Press: Berkeley, Los Angeles, London, 1986; Chapter 6.

(3) Miyazaki, T.; Hiraku, T.; Fueki, K.; Tsuchihashi, Y. *J. Phys. Chem.* ***1991****, 95*, 26.

(4) Kumada, T.; Inagaki, H.; Nagasawa, T.; Aratono, Y.; Miyazaki, T. *Chem. Phys. Lett.* ***1996****, 251*, 219.

(5) Miyazaki, T.; Kitamura, S.; Morikita, H.; Fueki, K. *J. Phys. Chem.* ***1992****, 96*, 10331 and references therein.

(6) Rushbrooke, G. S.; *Introduction to Statistical Mechanics*; Clarendon: Oxford, 1951.

(7) DeRose, E. F.; Gislason, E. A.; Sabelli, N. H.; Sluis, K. M. *J. Chem. Phys.* ***1988****, 88*, 4878.

(8) Nakano, F. Private Communication.

(9) Kagan, Y.; Klinger, M. I. *J. Phys.* ***1974***, *C7*, 2791.

(10) Kiefl, R. F.; Kadono, R.; Brewer, J. H.; Luke, G. M.; Yen H. K. *Phys. Rev. Lett.* ***1989***, *62*, 792.

(11) Kadono, R.; Kiefl, R. F.; Ansaldo, E. J.; Brewer, J. H.; Celio, M.; Kreitzman, S. R.; Luke, G. M. *Phys. Rev. Lett.* ***1990***, *64*, 665.

Table 1: Parities of wave functions on exchanging each proton in a H_2 molecule or a H_2^- anion.[a]

	Vibration	Rotation	Electron	Nuclear Spin	Total
para - H_2	sym.	sym.	sym.	anti.	anti.
ortho - H_2	sym.	anti.	sym.	sym.	anti.
para - H_2^-	sym.	anti.	anti.	anti.	anti.
ortho - H_2^-	sym.	sym.	anti.	sym.	anti.

[a] sym. and anti. represent symmetric and antisymmetric of wave functions, respectively.

Table 2: Decay rate of H_2^- anions and amounts of H_2^- anions and H atoms in X-rays-irradiated p-H_2 at 4.5 K.

Irradiation time (min.)	17	150
Decay rate[a] (arb. unit)	0.087	0.056
Amount of H_2^- (arb. unit)	0.43	3.5
Amount of H (arb. unit)	2.5×10^3	2.3×10^4

[a] Obtained by the kinetic plot of pseudo-first-order reaction for the data.

Figure Legend

Figure 1. ESR spectra of H_2^- anions in γ-rays-irradiated solid parahydrogen at 4.2 K measured in a wide range of magnetic field. The peaks, indicated by B1, B2, B3 and B4, are attributed to $|I=1, I_Z=0\rangle$, $|0, 0\rangle$, $|1, 1\rangle$ and $|1, -1\rangle$ states of H_2^- anions, respectively.

Figure 2. The amount of H_2^- anions in γ-irradiated solid p-H_2 as a function of storage time at 4.2 K. (●, ■, ▲) B1 (o-H_2^-) peak in Figure 1, (○, □, △) B2 (p-H_2^-) peak in Figure 1. Circles, squares and triangles are the results in three different samples.

Figure 3. Ratios of the amounts of p-H_2^- (●, ■, ▲) and o-H_2^- (○, □, △) to the total amount of H_2^- anions against storage time at 4.2 K. (see text)

Figure 4. Initial amount of H_2^- anions in γ-irradiated solid p-H_2 at 4.2 K as a function of concentrations of D_2 + HD molecules. (▲) B1 (o-H_2^-) peak in Figure 1, (▽) B2 (p-H_2^-) peak in Figure 1. It is pointed out that, in any sample, a concentration of HD is 0.03 mol % which is obtained from natural abundance of D (0.015 mol %) in H.

Figure 5. Relative amount of H_2^- anions in γ-irradiated p-H_2-D_2 mixtures against storage time at 4.2 K. (●, ■, ▲) o-H_2^- and (○, □, △) p-H_2^-, obtained from B1 and B2 peaks in Figure 1. Circles, squares and triangles correspond to the D_2 + HD concentrations at 0.03, 0.04 and 0.13 mol %, respectively. It is pointed out that, in any sample, a concentration of HD is 0.03 mol % which is obtained from natural abundance of D (0.015 mol %) in H. All the amounts at t=0 are normalized to 10.

Figure 6. Time-course of the total amount of H_2^- anions in γ-irradiated solid p-H_2 at 4.2 K (●, ■, ▲) and 2.2 K (◇, ▽). The experiments were done for three samples at 4.2 K and for two samples at 2.2 K.

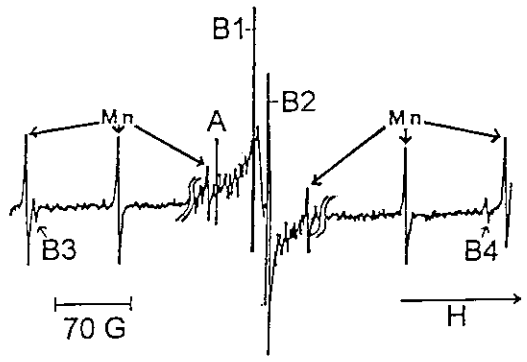

Fig. 1

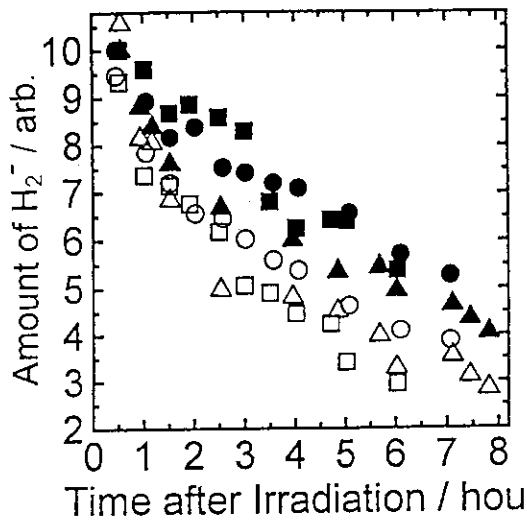

Fig. 2

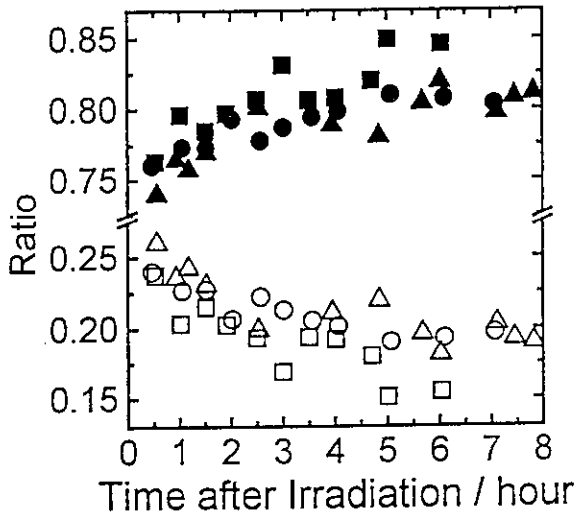

Fig. 3

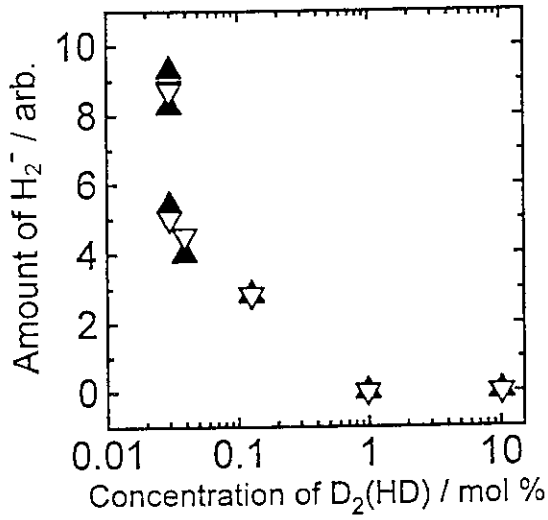

Fig. 4

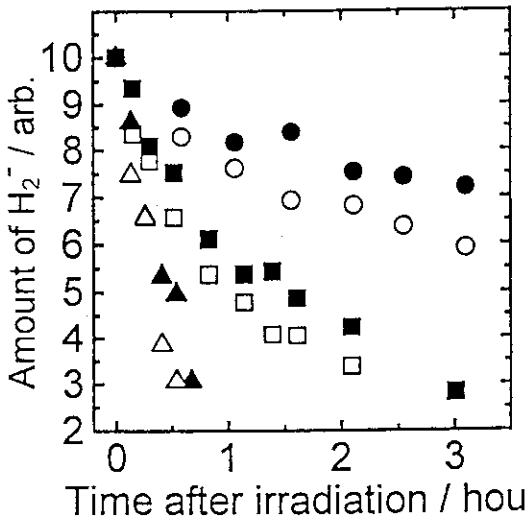

Fig. 5

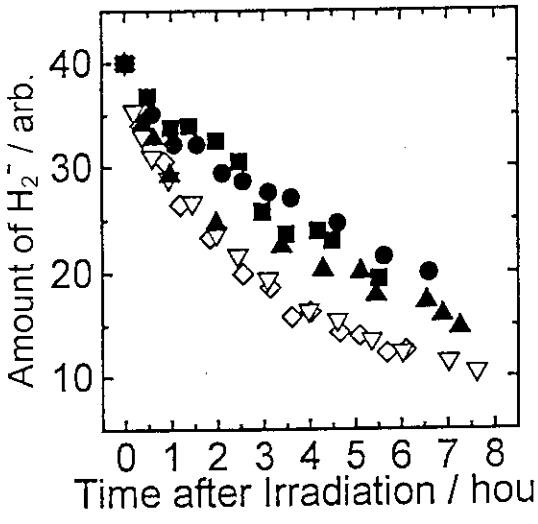

Fig. 6

5. Deuterium Isotope Effects on Rotation of Methyl Hydrogens −An ESR study of Dimethylether Radical Cations−

Masaru Shiotani,* Nobuyuki Isamoto and Michiro Hayashi
Faculty of Engineering , Hiroshima University ,
Higashi-Hiroshima 739 , Japan

An ESR study was carried out for deuterium isotope effects on structure of dimethylether radical cations. Strong deuterium isotope effect has been observed for the methyl group conformation and rotation. For example, $CD_3OCHD_2^+$ gave a large ^1H hf splitting 8.8 mT at 4K. The result suggests the light hydrogen preferentially occupying the position parallel to the unpaired electron orbital of oxygen. The temperature-dependent hf splittings were interpreted in terms of a hindered rotation of the partially deuterated methyl group.

Use of selectively ^2D-labelled compounds is essential for an unequivocal assignment of ESR spectrum of organic radicals.[1-10] In addition the ^2D-labelling is expected to give rise to important effect on electronic and geometric structure of the radical because of the mass difference. A number of deuterium isotope effects on structure and reaction of organic radical ions have been studied.[5] However, only limited studies show clear isotope effects on structure. Here, we wish to report our recent ESR study which shows strong and clear deuterium isotope effects on conformation and rotations of methyl hydrogens. The effects are demonstrated using selectively deuteriated dimethy-ether radical cations.

Figure 1 shows the ESR spectra of six different deuterium labeled dimethylether radical cations which were generated and stabilized in a halocarbon matrix by ionizing radiation at 77K. In the spectra of the radical cations of $CD_3OCH_3^+$, $CD_3OCH_2D^+$, and $CD_3OCHD_2^+$ number of ^1H hyperfine (hf) lines decrease from 4 to 3 and 2 depending on that of light hydrogen, respectively. Interestingly, the ^1H hf splitting was found to increase with increasing in number of

* *To Whom correspondence should be addressed.*

deuteriums substituted from 4.3 mT for CH_3 to 5.2 mT for CH_2D and 6.2 mT for CHD_2 at 77K. The temperature-dependent ESR spectra were observed for the radical cations in the temperature range from 4 K to 100 K at which the radical cations undergo changes to neutral radicals. It was found that, for example, the ^1H hf splitting of $CD_3OCHD_2^+$ decreases with increasing temperature from

Table 1: Experimental ^1H and ^2D hfs splittings of ^2D- labeled dimethylether radical cations in CCl_3F at 77K

	^1H-hfsc (mT)	^2D-hfsc (mT)
$CH_3OCH_3^+$	4.3(6H)	-
$CH_3OCH_2D^+$	5.2(2H) 4.3(3H)	$0.5_5\pm0.0_4$
$CH_3OCD_3^+$	4.3(3H)	$0.6_0\pm0.0_4$
$CD_3OCH_2D^+$	5.2(2H)	$0.6_0\pm0.0_3$
$CD_3OCD_2H^+$	6.2(1H)	$0.6_0\pm0.0_3$
$CD_3OCD_3^+$	-	0.6_6

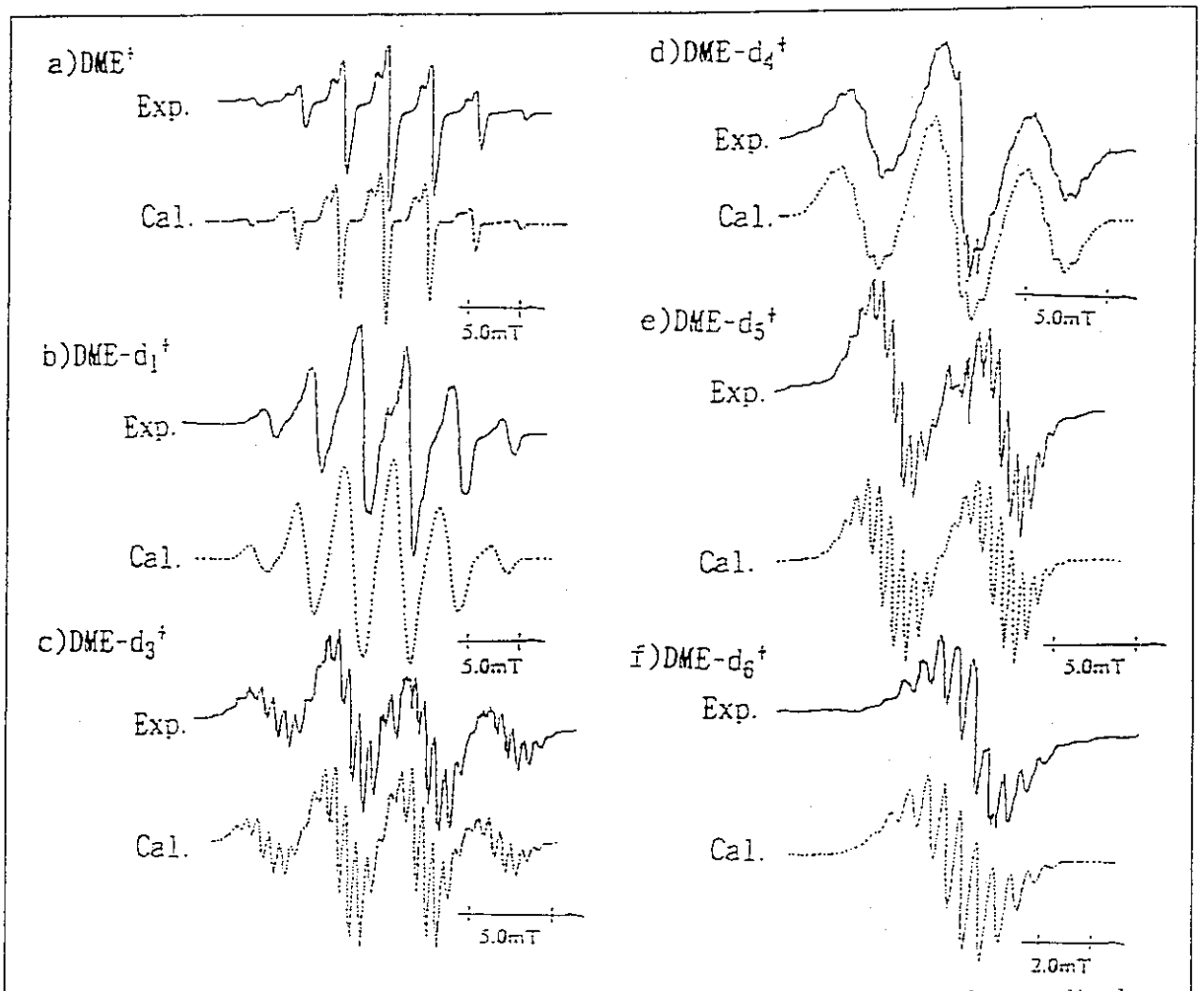

Figure 1: The ESR spectra of six different ^2D- labeled dimethylether radical cations in CCl_3F at 77K . The simulated spectra are shown with the dotted lines.

8.8 mT at 4 K to 6.2 mT at 80 K; above the temperature the hf splitting becomes almost constant up to 100 K (Figure 2). On the other hand, no appreciable temperature dependent ^{1}H hf splitting was observed for the ^{1}H hf splitting of the CH_3 group, *i.e.*, the splitting of 4.3 mT corresponds to the rotationally averaged value of $CH_3OCH_3^+$. These results lead us to conclude that the light hydrogen of the CHD_2 group in $CD_3OCHD_2^+$ takes a fixed position at 4 K and the light and heavy hydrogens (^{1}H and ^{2}D) can not be completely averaged out even at higher temperature of 100 K.

Using McConnell type of equation for β-proton, $a^{\beta}_{H} = B_0 cos^2\theta$, and the experimental splitting of 4.3 mT for the rotationally averaging, $< a^{\beta}_{H} > = 4.3$ mT, we have 8.6 mT for the proportional constant, B_0. Comparing with the experimental value value of 8.8 mT for the ^{1}H splitting of CHD_2, we can conclude that the light hydrogen (^{1}H) selectively occupies the $\theta = 0°$ position which is parallel to the unpaired electron orbital of oxygen constituting $CH_3OCHD_2^+$ (Figure 3).

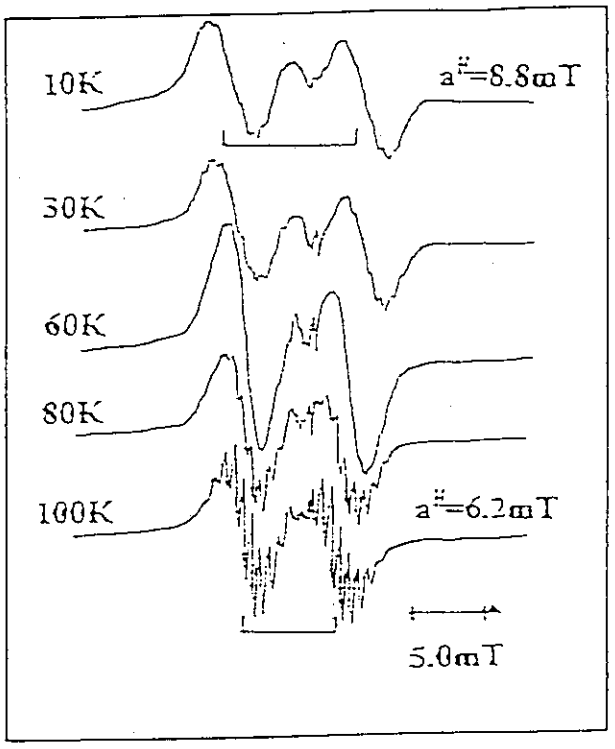

Figure 2: The temperature-dependent ESR spectra of $CD_3OCHD_2^+$ in CCl_3F.

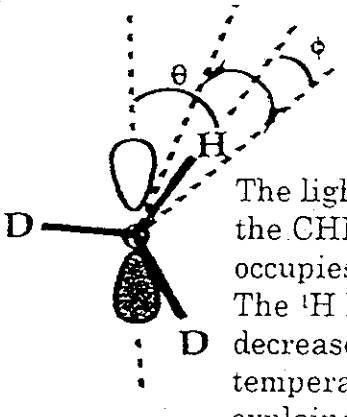

Figure 3

The light hydrogen (^{1}H) of the CHD_2 group selectively occupies the $\theta = 0°$ position. The ^{1}H hfs splitting decreases with increasing temperature. This can be explained by increasing in angle ϕ.

Hyperconjugation effect becomes maximum at the $\theta = 0°$ position. Through the effect the unpaired electron is transferred from the oxygen orbital to the hydrogen and the C-H bond should become weaker and elongated. The C-H bond strength is weaker than the C-D bond because the ^{1}H has two time smaller mass than ^{2}D. Weaker bond is easier to be elongated after the unpaired electron transfer. This can be explanation why the light hydrogen preferentially occupies the $\theta = 0°$ position.

The present temperature-dependent ^{1}H hyperfine splittings suggest that the exchange between ^{1}H and ^{2}D of the HD_2 group do not completely occur. One reason for this is that ^{1}H and ^{2}D are different particle in quantum mechanics: ^{1}H is *Fermion* with I (nuclear spin) = 1/2 and ^{2}D is *Boson* because with I = 1. According to Pauli exclusion principle the different particles can not be commuted to each other. Note that similar deuterium effect on the methyl hydrogen rotation has been reported for the partially deuteriated monofluoromethane radical cation of $CFDH_2^+$ by Knight and his coworker.[10]

It was observed in the present experiments that the ^{1}H hf splitting of the HD_2 group decreases with increasing temperature from 8.8 mT (4K) to 6.2 mT (100 K). This result can be successfully explained in terms of hindered rotation of the light hydrogen at $\theta = 0°$ position (Figure 3).

We summarize the present results as follows. 1) Strong and very clear deuterium isotope effects were observed for conformation and tunneling rotation of the methyl hydrogens of selectively deuteriated dimethylether radical cations: $CD_3OCHD_2^+$, $CD_3OCH_2D^+$, $CD_3OCH_3^+$ *etc.* 2) For example, $CD_3OCHD_2^+$ gives a large ^{1}H hf splitting of 8.8 mT at 4 K. 3) The result suggests the light hydrogen preferentially occuping the position parallel to the unpaired electron orbital of oxygen. 4) The splitting degreases with increasing temperature from 8.8 mT (4.2 K) to 6.2 mT (80 K), which is interpreted in terms of a hindered rotation of the partially deuteriated methyl group. 5) In contrast to the case of CH_3 group in $CH_3OCH_3^+$[11], the tunneling exchange between the light and heavy hydrogens of the CHD_2 and CH_2D group is ruled out.

Acknowledgment: The present study was partially supported by JSPS Program for Supporting University Industry Cooperation Research Project.

References

1) M. Shiotani, Mag. Res. Rev. 12, 33 (1987).
2) M. Shiotani and H. Yoshida, "ESR of radical ions",*CRC handbook of Radiation Chemistry* (*ed.* Y. Tabata), Chap. VIII.C, CRC Press, pp. 440-67 (1991).
3) A. Lund and M. Shiotani, (*eds*), "Radical ionic systems - Properties in condensed phases", Kluwer Academic Publisher (Dordrecht) , pp. 1- 496 (1991).
4) M. Lindgren, M. Shiotani, Chap. I.5 in *ref.3*, pp. 125 - 150 (1991).
5) M. Shiotani, A. Lund, Chap. I.6 in *ref.3*, pp. 151 - 176 (1991).
6) M. Shiotani, M. Lindgren, and T. Ichikawa, *J. Am. Chem. Soc.*, 112, 967 (1990).
7) M. Shiotani, K. Komaguchi, J. Ohshita, and M. Shikawa, *Chem. Phys. Lett.* 188, 93 (1992).
8) K. Komaguchi, M. Shiotani, M. Ishikawa, and K. Sasaki, *Chem. Phys. Lett.* 200, 580 (1992).
9) M. Lindgren, K. Komaguchi, and M. Shiotani, *J. Phys. Chem.*, *98*, 8331 (1994).
10) L.B. Knight, B.W. Gregory, D. W. Hill, et al., *J. Chem. Phys.* 94, 67 (1991).
11) T. Shida, T. Momose, and, M. Matsushita Chap. II.6 in *ref.3*, pp. 177 - 193 (1991).

6. Tunneling Hydrogen-atom Abstraction from Partially-deuterated Alkanes

Tsuneki Ichikawa and Koh-ich Kagei

Division of Molecular Chemistry, Graduate School of Engineering,
Hokkaido University, Sapporo, 060 Japan

Hydrogen-atom abstraction from alkane molecules is one of the simplest chemical reactions so that it has been extensively studied both experimentally and theoretically. For example, Evans and Polanyi studied the abstraction by methyl radicals and found so-called linear free energy relationship, that is, the activation energy for hydrogen abstraction is proportional to the dissociation energy of a C-H bond.[1]

The hydrogen abstraction proceeds even in cryogenic solids. Hydrogen or deuterium atoms can migrate in a cryogenic solid to abstract hydrogen atoms from solute alkane molecules. Since the activation energy for the abstraction ranges between 2600 K and 4000 K, and the pre-exponential factor A of the Arrhenius equation $k=A\exp(-E_a/RT)$ is a order of 10^{10}dm^3/mol•s, the lifetime of the hydrogen or deuterium atoms at 77 K is estimated to be more than 1 hr. However this is not the case. Because of the quantum-mechanical tunneling of C-H hydrogen, the lifetime is several orders of magnitude shorter than the expected value.

An alkane molecule has several intramolecular sites with different rates of hydrogen-atom abstraction. The activation energy for the hydrogen-atom abstraction decreases in the order of primary, secondary and tertiary carbon atoms, so that the tertiary alkyl radicals are expected to be preferentially generated by hydrogen-atom abstraction from branched alkanes. This is true for hydrogen-atom abstraction in liquid at room temperature. The hydrogen-atom abstraction from the secondary and the tertiary carbon are 4.8 and 40 times faster than tat from the primary carbon, respectively.[2] However the hydrogen-atom abstraction in cryogenic solids does not obey this rule. Willard et al. found that γ-irradiation of 3-methylpentane at 77 K caused selective formation of, not the tertiary 3-methyl-3-pentyl radical but the secondary 3-methyl-2-pentyl radical.[3] They also found that hydrogen-atom abstraction by hydrogen atoms generated by photolysis of HI also caused selective formation of the 3-methyl-2-pentyl radical.[4] Ichikawa and Ohta confirmed these results by using pertially-deuterated 3-methylpentane. They also found that the 3-methyl-3-pentyl radical was selectively generated when the hydrogen atoms of the secondary carbon atoms were replaced by deuterium atoms.[5,6] Although these results strongly suggests selective hydrogen-atom abstraction from, not the tertiary carbon, but the penultimate

secondary carbon, the other possibilities such as intermolecular conversion of the initially-generated radicals to the 3-methyl-2-pentyl radical and the selective formation of the 3-methyl-2-pentyl radical from the ionized or excited 3-methylpentane can not be ruled out. We have studied the hydrogen-atom abstraction from linear and branched alkane molecules by hydrogen or deuterium atoms in perdeuterated organic matrices at 77 K and found that the hydrogen-atom abstraction preferentially took place at the penultimate secondary carbon. [7,8,9] However, because of the overlapping of the ESR spectra of different alkyl radicals, identification of the radical species was not necessarily rigorous.

The present study was aimed at determining the preferential site for partially-deuterated alkane molecules in deuterated methanol matrix at 77 K by analyzing the ESR spectra of resultant alkyl radicals. It was found that the rate of hydrogen-atom abstraction is determined not only by the activation energy but also classical factors but also by a quantum-mechanical factor, probably by the degree of overlapping of the atomic wave functions of an initial reactant state and final product states.

Partially-deuterated alkanes synthesized were $CD_3CH_2CH_2CH_2CH_2CD_3$, $CH_3CH(CD_3)CH_2CH_3$, $CH_3CH(CD_3)CH_2CH_2CH_3$ and $CH_3CH_2CH(CD_3)CH_2CH_3$. The concentration of solute alkanes was about 2 mol%. The deuterium atoms were generated at 77 K either by γ-radiolysis of the deuterated matrix or by photo-ionization of triphenylamine followed by dissociative capture of ejected electrons by DCl. The hydrogen-atom abstraction proceeded through quantum-mechanical tunneling of the C-H hydrogen atoms, so that the deuterium atoms selectively abstracted the hydrogen atoms of the solute molecules. The intramolecular conversion of the initial alkyl radicals to another ones was confirmed to be prohibited at least at 77 K, so that the location of an unpaired electron of the product radical was the same as that of a hydrogen-abstracted carbon atom.

Analysis of the ESR spectra revealed that the hydrogen-atom abstraction preferentially takes place at the penultimate carbon atoms. Although the penultimate tertiary carbon atoms of $CH_3CH(CD_3)CH_2CH_3$ and $CH_3CH(CD_3)CH_2CH_2CH_3$ are hydrogen-atom abstracted, the antepenultimate tertiary carbon atoms of $CH_3CH_2CH(CD_3)CH_2CH_3$ are not hydrogen-atom abstracted. Substitution of one of two methyl substituents to ethyl substituent therefore drastically decreases the reactivity of the tertiary carbon atom. Since the activation energy for hydrogen-atom abstraction is the same for the penultimate and antepenultimate tertiary carbon, the low reactivity of the antepenultimate tertiary carbon atom obviously arises from some kind of steric hindrance toward hydrogen-atom abstraction. We propose that the decrease in the rate of hydrogen-atom abstraction arises from the decrease in the

Frank-Condon factor of chemical reaction or the degree of the overlap of atomic wave functions between the initial alkane state and the final vibrationally-excited alkyl radical state. Since the reaction is exothermic, the heat of reaction must be absorbed mainly as vibrational and rotational energies of the resultant HD and alkyl radical. The efficiency of heat absorption by the alkyl radical is proportional to the degree of the overlap of atomic wave functions between the initial cold alkane molecule and the final hot alkyl radical. The degree of the overlap increases with increasing atomic displacement between the initial and the final states. The displacement is forced to be reduced in a rigid matrix due to steric hindrance to the motion of alkyl substituents bonded to the carbon atom to be hydrogen-atom abstracted. The steric hindrance increases with increasing number and length of the alkyl substituents, so that the reactivity for the antepenultimate tertiary carbon atom of 3-methylpentane with -CH_2CH_3 and -CH_3 substituents is much lower than that of the penultimate secondary carbon atom with -H and -CH_3 substituents. On the other hand, the reactivity of the penultimate tertiary carbon atom of 2-methylbutane or 2-methylpentane is comparative to that of the secondary carbon atoms, since -CH_2CH_3 is replaced with smaller -CH_3.

One of the simplest explanations for the steric hindrance would be that two CH_2CH_3- prevent the approach of a deuterium atom to the tertiary C-H, whereas not for -CH_3. However, it is evident from the molecular structures that the two substituents do not highly protect the tertiary C-H. Another explanation would be that the deformation of the C-C-C bond is necessary for attaining the minimum activation energy. However a molecular orbital calculation of the potential surface for hydrogen-atom abstraction showed that no deformation of the C-C-C bond is necessary for the reaction path with the minimum activation energy.

References

1) M.G. Evance and M. Polanyi, Trans. Faraday. Soc., 34, 11 (1938)
2) W.A. Pryor and J.P. Stanley, J. Amer. Chem. Soc. 93, 1412 (1971)
3) D. Tims, J.E. Willard, J. Phys. Chem., 73, 2403 (1969)
4) ibid., J. Amer. Chem. Soc. 91, 3406 (1969)
5) T. Ichikawa, N. Ohta, J. Phys. Chem., 81, 560 (1977).
6) T. Ichikawa, N. Ohta, Radiat. Phys. Chem., 29, 429 (1987).
7) T. Ichikawa, H. Yoshida, J. Phys. Chem., 96, 7656 1992)
8) idem, ibid, 96, 7661 (1992)
9) H. Koizumi, M. Hashino, T. Ichikawa, H. Yoshida, Radiat. Phys.ibid., 40, 145 (1992)

7. Chemical Reactions of Tritium Atom Produced in Super-fluid ^{3}He-^{4}He Mixture

Yasuyuki Aratono[1)], Takayuki Kumada[1)], Kenji Komaguchi[1)]
Takuro Matumoto[2)] and Tetsuo Miyazaki[1,2)]

1) Advanced Science Research Center, Japan Atomic Energy Research Institute, Tokai-mura, Ibaraki-ken 319-11, Japan
2) Department of Applied Chemistry, School of Engineering, Nagoya University, Furo-cho, Chikusa-ku, Nagoya 464-01, Japan

Tritium reaction in superfluid helium was studied at 1.3 K. Tritium atom(T) was produced in the solution by the nuclear reaction of ^{3}He(n,p)^{3}H. The isotope effect for $T + H_2 \rightarrow HT + H$ and $T + D_2 \rightarrow DT + H$ was obtained to be 185. The value suggests that tunneling abstraction is a predominant process for HT and DT formation.

1. Introduction

Many peculiar properties of normal- and super-fluid liquid helium(^{3}He and ^{4}He) arising from their quantum properties have been attracting many scientists. However, the studies have been mainly focused on the physical aspects[1)]. The one of the most difficult points upon the study of chemical or physical behaviors of atoms or ions in liquid helium medium is how to introduce reactive species in it.

It is well known that the mixture of liquid ^{3}He and ^{4}He shows normal- and super-fluid character depending on the composition and temperature, as is presented in Fig. 1. Helium-3 has a very large activation cross section for thermal neutron(5.33 x 10^3 barns) and gives recoil T, which is one of the hydrogen isotopes, according to the following nuclear reaction, ^{3}He(n, p)T. That is to say, the mixture has two roles, reaction medium and

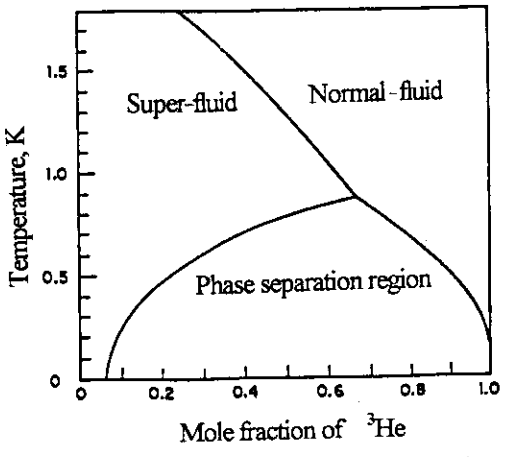

Fig. 1 Phase diagram of ^{3}He-^{4}He mixture under saturated vapor pressure.

T source. It is very interesting to investigate the chemical reactions of T in the normal- and super-fluid ^3He -^4He mixtures from the viewpoint of how the chemical reaction proceeds in such a quantum liquid. In the present experiment, the super-fluid solution was first selected as a reaction medium because of its characteristic properties compared with the normal-fluid.

2. Experimental

Helium-3 was purchased from Isotec Inc. and isotopic enrichment was more than 99.9 atomic %. Tritium content in ^3He was less than 10^{-11} atomic % and was under detection limit for the present T counting system. Deuterium gas(D_2) was also a product of Isotec Inc. and isotopic content of D was more than 99.6%. The purity of other gases was more than 99.999 %.

The mixture of ^3He:^4He=0.282:0.718 at liquefied state at 1.3 K was introduced into reaction vessel of Pyrex glass flask(about 3.8 l) with quartz tube(6 mm in inner diameter, 1 m in length). The pre-determined amount of H_2 and/or D_2 were added into the mixture in some cases.

Deuterization of the inner wall of the quartz tube was carried out by heating for 1 day at 1273 K under D_2 pressure of 4.4×10^4 Pa. The conversion of OH group was monitored by IR spectrometer. About 60 % of OH group was converted into OD group.

Thermal neutron irradiation was performed at JRR-2 of Japan Atomic Energy Research Institute for about 50 hrs at 1.3 K. As the irradiation port was designed for neutron scattering experiment, the γ -ray dose rate is very low so that the secondary effect caused by γ -ray can be neglected. The thermal neutron flux was about 10^{11} m^{-2} sec^{-1}. The photograph of the liquefied sample under neutron irradiation is presented in Fig. 2. The white part is the irradiation window of the cryostat and dark part of the center is the super-fluid sample absorbing thermal neutron and the reaction occurs in it.

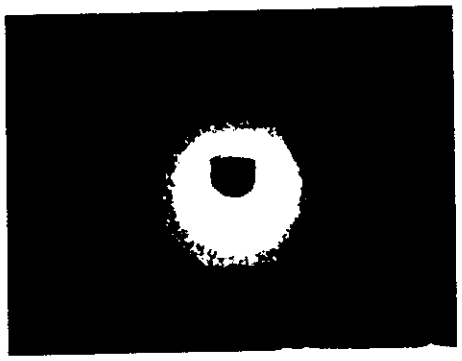

Fig. 2 Photograph of the sample under irradiation.

The irradiated sample was analyzed by radio-gaschromatograph equipped with a gas-flow proportional counter. The reaction products, HT, DT, and T_2 were separated at 77 K using the column of γ-alumina coated with Fe_2O_3. Typical gas-chromatogram is shown in Fig. 3. A complete separation is obtained for HT and DT.

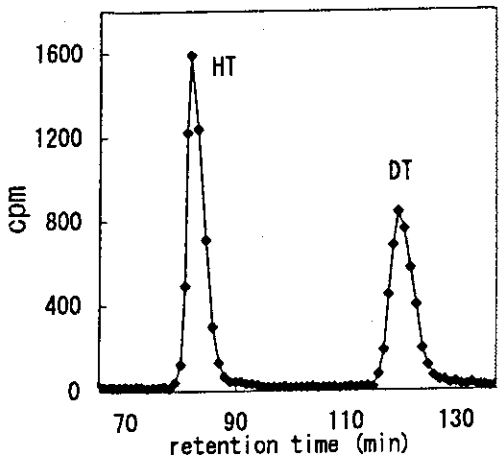

Fig. 3 Radio-gaschoromatogram of HT and DT

3. Results and Discussion

3.1 Distribution of reaction products and isotope effect

Table 1 shows the yield of reaction products expressed as the percentage of the radioactivity of tritiated product against total

Table 1 Distribution of reaction products

Additives	HT(%)	DT(%)	T_2(%)	Remarks
none	100	0	0	Irradiated at JRR-2
none	97.9	0	2.1	Irradiated at JRR-3*)
none	90.6±2.8	9.5±2.8	0	Inner wall deuterated
H_2(1 vol%)	100	0	0	Inner wall deuterated
D_2(1 vol%)	59.9	40.1	0	
H_2, D_2(1vol%)	94.6±1.1	5.4±1.1	0	H_2/D_2=1/9

*) Result from JRR-3 experiment. The flux of thermal neutron at JRR-3 is few times larger than that at JRR-2.
Other results are all from JRR-2 experiments.

radioactivity . A very small amount of T(<0.1%) was detected in the condensate trapped at 77 K but was neglected in the discussion. The main products are tritiated hydrogen isotopes, HT and DT. In JRR-3 experiment, small amount of T_2, which was formed by the recombination reaction of T, was observed in the sample without additive.

It is well known as wall effect that T formed near or migrating near wall abstracts H atom of OH group, which is on the surface of the inner wall, to give HT. Thus, it was estimated by the inner wall deuterated sample. As is seen in the Table, the yield of DT is 9.5±2.8 % which suggests that about 90 % of T reacts within the liquid helium medium.

The effect of D_2 addition is in contrast to the result in H_2

addition. In spite of no H_2 addition, about 60 % of T is observed as HT which is much higher even if the wall effect is taken into consideration. The most plausible source of hydrogen is impurity included D_2 gas. In any case, the results suggest a very large isotope effect for abstraction of H and D by T.

A clear evidence of preferential abstraction of H to D by T was obtained in the reaction system of H_2-D_2 addition. The yield of HT is 18 times larger than that of DT, though the amount of H_2 is less than that of D_2 by a factor of 9. The isotope effect calculated from Table 1 is 185, where the wall effect was taken into account.

3.2 Reaction mechanism

The possible pathways leading to the formation of HT and DT in H_2-D_2 system can be considered as follows.

(1) formation of tritium

Tritium atom is formed through the nuclear reaction,

$$^3He + n \rightarrow T^* + p. \quad (1)$$

Energy released by the reaction(Q value) is distributed to T^* and proton, where T^* means translationally excited T. Therefore, an initial kinetic energy of T^* is calculated to be 192 keV.

(2) thermalization of T^*

Energetic tritium(T^*) looses its kinetic energy by the successive collision with a large amount of ^3He and ^4He and is finally thermalized.

$$T^* + He \rightarrow He^* + T \quad (2)$$

(3) formation of HT and DT

Two pathways are considered to be possible as the formation of HT and DT. One is the abstraction reaction of thermalized T with H_2 and D_2 (reactions 3 and 4) and another one is the reaction of the thermalized T with H and D (reactions 7 and 8) formed by the energy transfer process from the excited He(He^*) (reactions 5 and 6), which is produced along the track of the high LET energetic tritium.

$$T + H_2 \rightarrow HT + H \quad (3)$$

$$T + D_2 \rightarrow DT + H \quad (4)$$

$$He^* + H_2 \rightarrow H + H \quad (5)$$

$$He^* + D_2 \rightarrow D + D \quad (6)$$

$$T + H \rightarrow HT \quad (7)$$

$$T + D \rightarrow DT \quad (8)$$

As for the reactions (5) and (6), there is no experimental

and theoretical studies on the isotope effect for the formation of H and D. Therefore, it was speculated based on the experimental results obtained by some of the authors in γ-ray irradiated Xe-H_2-D_2 (H_2+D_2 =1 mol %) at 4.2 K[2] and X-ray irradiated Ar-H_2-D_2(H_2+D_2) =1 mol %) at 4.5 K[3]. In these systems, the H and D produced by γ- or x-ray radiolysis cannot diffuse through the matrix. The isotope effect in the former is 1.3 and the latter about 1. Hyden et al. studied the recombination reactions of H + D + ^{4}He → HD + ^{4}He and D + D + ^{4}He → D_2 + ^{4}He in the gas phase at 1 K, where H and D are formed by rf discharge in gas phase and confined by liquid helium coated wall[4]. The rate constants are identical each other. Thus, isotope effect in the reactions of (7) and (8) is presumed to be small.

In conclusion, the very large isotope effect obtained in the present experiment is anticipated to be mainly ascribed to the tunneling abstraction through the reactions (3) and (4).

3.3 Comparison of the isotope effects

The isotope effect for T + H_2(D_2) → HT(DT) + H(D) has been examined by some workers. Table 2 summarizes the results including the present data.

Table 2 Isotope effects for T + H_2(D_2) → HT(DT) + H(D)

Phase	Temp. (K)	isotope effect	Remarks
Gas[5]	Room	2.7	K.E.=192 keV[a] Scavenged
Gas[5]	Room	1.55±0.06	K.E.=192 keV[a] Unscavenged
Gas[6]	Room	0.98±0.03	K.E.=2.8 eV[b]
Liquid*)	1.3	185	K.E.=192 keV[a]
Solid[2]	77	7	K.E.=2.7 MeV[c]

K.E.: Initial kinetic energy of T produced by the following three processes.

a) ^{3}He(n,p)T, b) TBr--(photolysis)--→T + Br, c) ^{6}Li(n,α)T

*): Present result

Though the isotope effects in the gas phase somewhat depend on the experimental conditions, the values lie below 3. On the other hand, the value, 7, obtained by some of the present authors at 77 K in highly moderated Xe-H_2-D_2 system[2] is much higher than those in the gas phase and suggests the contribution of the

tunneling abstraction reaction. The present result exceeds by about two orders of magnitude over the gas phase values and is close to those of H and D in the solid hydrogen at around 4 K where the tunneling abstraction by hydrogen isotopes was well established[7].

4. Conclusion

The abstraction of H and D by T was studied with an advantage of direct formation of reactive species in super-fluid helium medium by nuclear reaction. The tunneling process was proposed for the formation of HT and DT based on the very large isotope effect. Gordon et al. investigated the behavior of H and D atoms trapped in super- and nomal- fluid helium by ESR spectroscopy at 1.8 - 4.2 K[8]. Though they report the tunneling process in such a medium, the reaction proceeds in the solid phase, as they describe in the paper. The present paper is the first experimental report on the chemical reaction in liquid helium so far as we referred to the literatures.

5. Acknowledgements

The authors would like to thank Mr. Minagawa and Mr. Shimojyou of Neutron Scattering Laboratory of Japan Atomic Energy Research Institute for their many advices in neutron irradiation. The present research was supported in part by a Grant in Aid for Scientific Research from the Japanese Ministry of Education, Science and Culture.

References

1) "Proceedings of the 128th WE-Heraeus-Seminor on Ions and Atoms in Superfluid Helium" Zeitschrift fur Physik B 98(1995).
2) T. Miyazaki, Y. Fujitani, M. Shibata, K. Fueki, N. M. Masaki, Y. Aratono, M. Saeki, and E. Tachikawa, Bull. Chem. Soc. Jpn., 65, 735(1992).
3) K. Komaguchi, private communidation.
4) M. E. Hayden and W. N. Hardy, J. Low Temp. Phys., 99(5/6), 787(1995).
5) J. K. Lee, B. Musgrave, and F. S. Rowland, J. Chem. Phys., 32, 1266(1960).
6) C. C. Chou and F. S. Rowland, 46, 812(1967).
7) T. Miyazaki, Radiat. Phys. Chem., 37(5/6), 635(1991).
8) E. B. Gordon, A. A. Pele'menev, O. F. Pugachev, and N. V. Khmelenko, Sov. J. Low Temp. Phys., 11(6), 307(1985).

8. Tunneling Effect in Antioxidant and Prooxidant Reactions of Vitamin E

Shin-ichi Nagaoka, Masayo Inoue, Chiho Nishioka, and Kazuo Mukai
Department of Chemistry, Faculty of Science, Ehime University, Matsuyama 790-77, Japan

Abstract: Kinetic studies of the antioxidant and prooxidant reactions of vitamin E have been carried out. The tunneling effect plays an important role in the antioxidant reaction, but not in the prooxidant reaction.

Introduction

Figure 1 shows a plot of the life span potential vs the rate of oxygen consumption per unit body weight in mammalian species.[1] Agelessness, which is one of the ultimate hopes of the human beings, is located at the infinity of the ordinate. As shown in Figure 1, the life span potential is inversely proportional to the rate of oxygen consumption. Although oxygen is essential to life in mammalian species, it produces a side effect and shortens the lifetime. From Figure 1, we can regard aging as an evidence of living. For when the rate of oxygen consumption equals to zero (then he/she is dead!), he/she can get agelessness and eternal life.

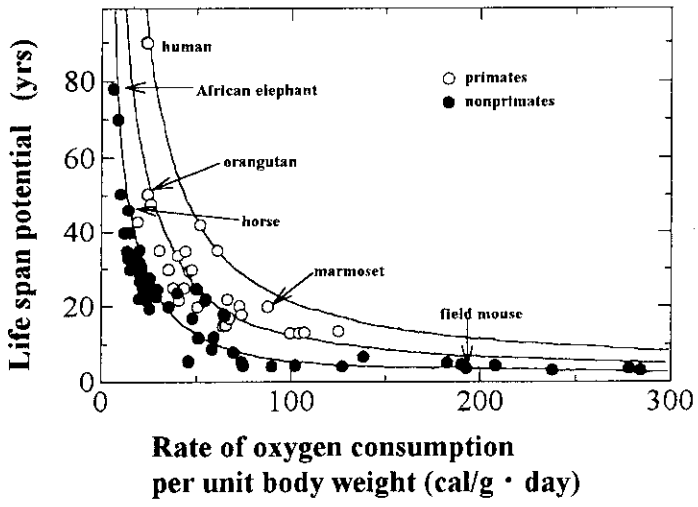

Figure 1. Plot of life span potential vs rate of oxygen consumption per unit body weight in mammalian species.

Why does oxygen shorten his/her lifetime? Recent studies show that lipid peroxyl radicals (LOO·'s) formed from reactions of lipids and oxygen are one of the causes of aging. However, the living body has a function to scavenge LOO· and to prevent aging. That is the so-called antioxidant reaction of vitamin E. We can find the evidence for the function of vitamin E in the fact that the life span is proportional to plasma level of vitamin E.[1] From these facts, one can see that the study of the antioxidant reaction and the understanding at molecular level require immediate attention because of the present and future aging society.

Figure 2 shows the scheme of production of LOO· and the antioxidant reaction of vitamin

E (TocH).[2-4] At first, a radical (L·) is formed from lipid usually by an attack of radicals, light, heat, irradiation, or metal. L· reacts with oxygen to produce LOO·. The reaction of TocH and LOO· results in the production of hydroperoxide (LOOH) and vitamin E radical (Toc·). TocH is regenerated by the reaction of Toc· and vitamin C at the interface between the cell membrane and the water phase.

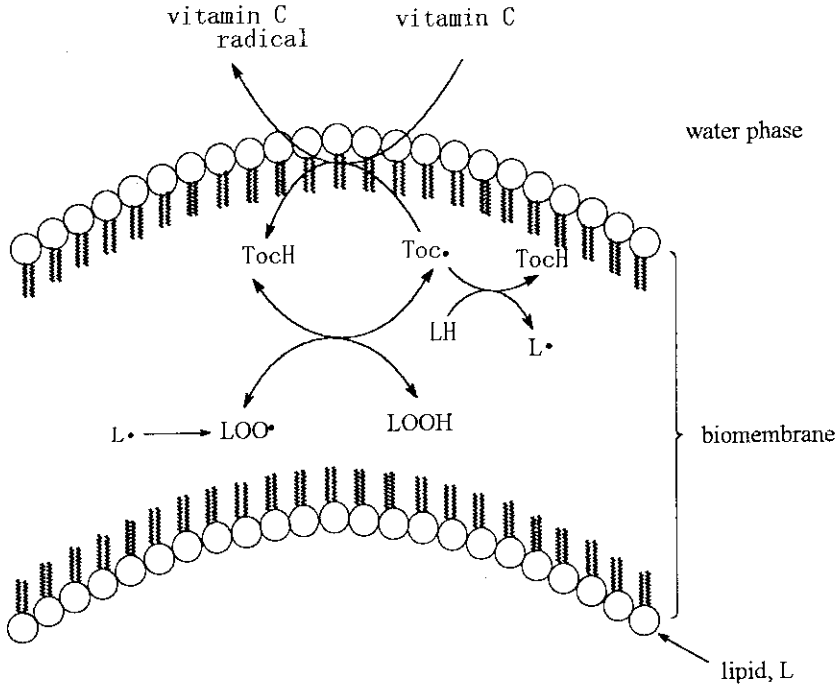

Figure 2. Scheme of antioxidant and prooxidant reactions of TocH.

Figure 3 shows the molecular structures of natural TocH's, which have a hydroxychroman ring and a phytyl side chain. The side chain stabilizes TocH in the cell membrane.

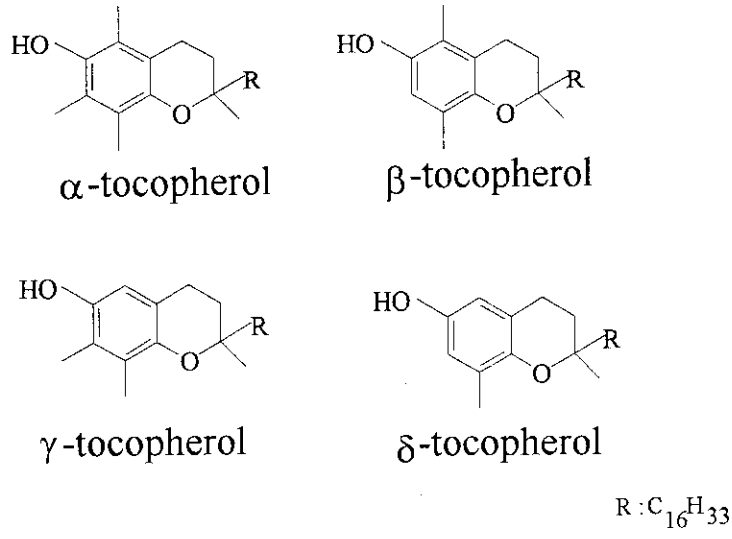

Figure 3. Molecular structures of natural TocH's.

These TocH's differ from one another only in the number and position of the methyl groups on the aromatic ring. α-TocH, which is fully methylated, is the most plentiful and the most biologically active in these four molecules and is selectively transported *in vivo* by α-TocH transfer protein.[5]

As shown in Figure 2, the antioxidant reaction of TocH is essentially a proton or hydrogen transfer reaction such as,

$$\mathrm{TocH} + \mathrm{LOO}\cdot \rightarrow \mathrm{Toc}\cdot + \mathrm{LOOH} \qquad (1)$$

We proposed that the mechanism of reaction 1 is as follows.[6-11]

$$\mathrm{TocH} + \mathrm{LOO}\cdot \rightarrow [\mathrm{TocH}^{\delta+}\text{- - -}\mathrm{LOO}\cdot{}^{\delta-}] \quad \text{(partial electron transfer)}$$
$$\rightarrow [\mathrm{Toc}\cdot\text{- - -}\mathrm{LOOH}] \quad \text{(proton tunneling)}$$
$$\rightarrow \mathrm{Toc}\cdot + \mathrm{LOOH} \qquad (2)$$

In the initial stage of the reaction, TocH and LOO· approach each other and their electron clouds begin to overlap. TocH and LOO· are relatively susceptible to donating and accepting an electron, respectively. Thus, the final goal of this process is the transition state which has the property of the charge transfer species ([TocH^{+}- - -$\mathrm{LOO}\cdot{}^{-}$]). In reality, when TocH and LOO· approach each other to some extent ([$\mathrm{TocH}^{\delta+}$- - -$\mathrm{LOO}\cdot{}^{\delta-}$]), the proton tunneling takes place below the transition state. Finally, the Toc· and LOOH separate from each other. Both the electron transfer and the proton tunneling play important roles in reaction 1.

In order to confirm the above-mentioned mechanism of reaction 1, we have made kinetic studies of reaction 1 by means of the stopped-flow spectroscopy. The kinetic study of the reversal of reaction 1, which is one of the prooxidant reactions of vitamin E, has also been performed. From these results, we have examined the role of proton tunneling in the antioxidant and prooxidant reactions of vitamin E.

Antioxidant Reaction

The kinetic data of the antioxidant reaction were obtained with a Unisoku stopped-flow spectrophotometer Model USP-500. In the stopped-flow spectroscopy,[12] the two solutions are mixed very rapidly under a nitrogen atmosphere by injecting them into a tangential mixing chamber designed to ensure that the flow is turbulent and that complete mixing occurs. Beyond the mixing chamber there is an observation cell fitted with a stopping syringe, which moves back as the liquids flood in but comes up against a stop when a required volume (typically about 1 mL) has been injected. The reaction then continues in the thoroughly mixed solution and is monitored. One can also obtain a time-resolved absorption spectrum by means of the rapid scan option of the stopped-flow apparatus.

In order to gain experimental and theoretical understanding of the mechanism for the antioxidant reaction *in vivo*, it is desirable to study simple systems. In the present study, we have used 2,6-di-*t*-butyl-4-(4'-methoxylphenyl)phenoxyl (PhO·) as a model for LOO·.

$$\mathrm{TocH} + \mathrm{PhO}\cdot \xrightarrow{k_S} \mathrm{Toc}\cdot + \mathrm{PhOH} \qquad (3)$$

Here, PhOH stands for a phenol derivative.

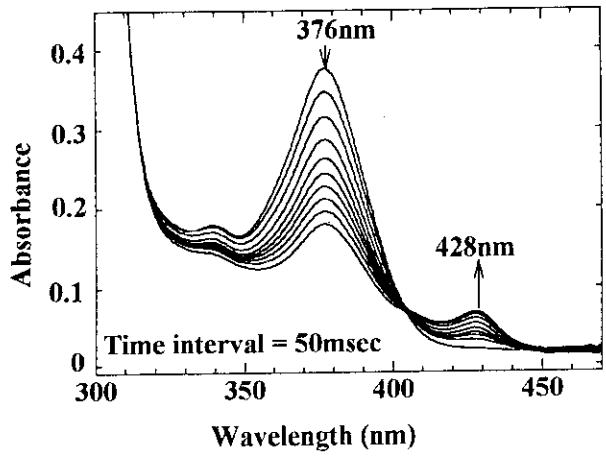

Figure 4. Change in absorption spectrum during reaction 3 in ethanol.

Figure 4 shows the change in absorption spectrum during reaction 3. The absorbances at 428 nm of Toc· and at 376 nm of PhO· increase and decrease, respectively, as reaction 3 proceeds. The pseudo-first-order rate constant (k_{obsd}) was determined by following a decrease in absorbance of PhO·. k_{obsd} is given by eq 4.

$$k_{obsd} = k_0 + k_s[TocH] \qquad (4)$$

k_0 denotes the rate constant for natural decay of PhO·. k_s stands for the second-order rate constant for reaction 3. [TocH] refers to the molar concentration of TocH. The rate parameters were obtained by plotting k_{obsd} against [TocH]. The relative values of k_s (α-TocH : β-TocH : γ-TocH : δ-TocH = 100 : 44 : 47 : 20) agree well with those obtained from studies of the reactivities of TocH's toward poly(peroxystyryl)peroxyl radicals (100 : 41 : 44 : 14) by the O_2 consumption method (reaction 1).[2]

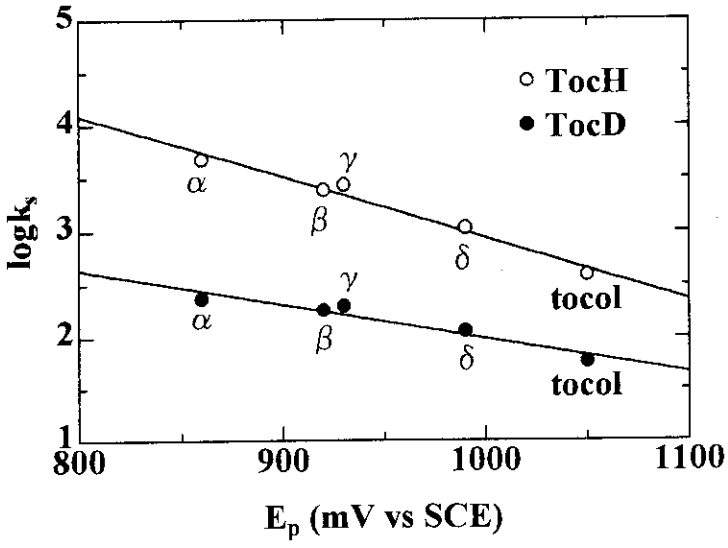

Figure 5. Plot of logk$_s$ in ethanol at 25 ℃ vs E_p of TocH.

Figure 5 shows a plot of $\log k_s$ at 25 ℃ vs the peak oxidation potential (E_p) of TocH.[7] k_s increases, as E_p decreases and the electron-donating capacity of TocH increases. The plot in Figure 5 is found to be linear. It is clearly more than coincidental that the k_s and E_p cluster near the straight line throughout the various systems studied. These facts indicate that the charge transfer plays an important role in reaction 1.

Figure 5 also shows a plot of $\log k_s$ for the reaction of deuterated TocH (TocD) and PhO· at 25 ℃ vs E_p. A substantial deuterium kinetic isotope effect on k_s is observed. Table I shows the ratio of k_s for TocH to that of TocD (k_s^H/k_s^D) at 25 ℃, the activation energy (E_{act}) obtained from k_s at 15-35 ℃, and the frequency factor (A_s). k_s^H/k_s^D amounts to 20.8 in α-TocH, and those of α-, β-, and γ-TocH's exceed the maximum semi-classical isotope effect (13).[13]

TABLE I: k_s^H/k_s^D at 25℃, E_{act} and $\log A_s$ for reaction 3 in ethanol, and E_p of TocH

	k_s^H/k_s^D	E_{act} (kJ/mol)	$\log A_s$	E_p vs SCE (mV)
α－TocH	20.8	18.0±0.8	6.8±0.2	860
α－TocD		22.2±2.1	6.2±0.4	860 [a)]
β－TocH	13.6	20.5±1.3	7.0±0.2	920
β－TocD		28.5±3.8	7.2±0.7	920 [a)]
γ－TocH	13.7	20.9±2.5	7.1±0.4	930
γ－TocD		28.9±1.7	7.3±0.3	930 [a)]
δ－TocH	9.30	23.8±0.4	7.2±0.1	990
δ－TocD		34.3±3.8	8.0±0.6	990 [a)]
tocol	6.76	26.8±1.3	7.3±0.2	1050
tocol－*d*		41.8±4.6	9.1±0.8	1050 [a)]

a) E_p in TocD was assumed to be equal to E_p in TocH.

The difference in E_{act} between tocol (6-hydroxychroman) and tocol-*d* also exceeds the maximum difference in zero-point energy (6.29 kJ/mol).[13] The ratio of A_s for tocol to that of tocol-*d* does not lie between 0.7 and 1.2 (criteria for semi-classical motion),[13] either. From these results, it is considered that proton tunneling plays an important role in reaction 1 as was suggested in Introduction. In the antioxidant reaction of TocH, the proton tunneling manifests itself in kinetic parameters determined here.

As the summary of the antioxidant reaction of vitamin E, we describe the mechanism on the basis of the results of molecular orbital calculations. Figure 6 shows the calculated contour map of the potential surface in a model reaction for reaction 1; in the calculation, phenol and CH_3OO· were used instead of TocH and LOO·, respectively; and the calculation method was AM1.[14] When TocH and LOO· approach each other to some extent, partial

electron transfer from TocH to LOO· takes place ([TocH $^{\delta+}$- - -LOO· $^{\delta-}$] in Figure 6). However, before [TocH $^{\delta+}$- - -LOO· $^{\delta-}$] reaches the transition state ([TocH^{+}- - -LOO·$^{-}$] in Figure 6), proton tunneling occurs, and the Toc· and LOOH separate from each other. From Figure 6, it is seen that the tunneling allows the proton to cut a corner on the potential energy surface.

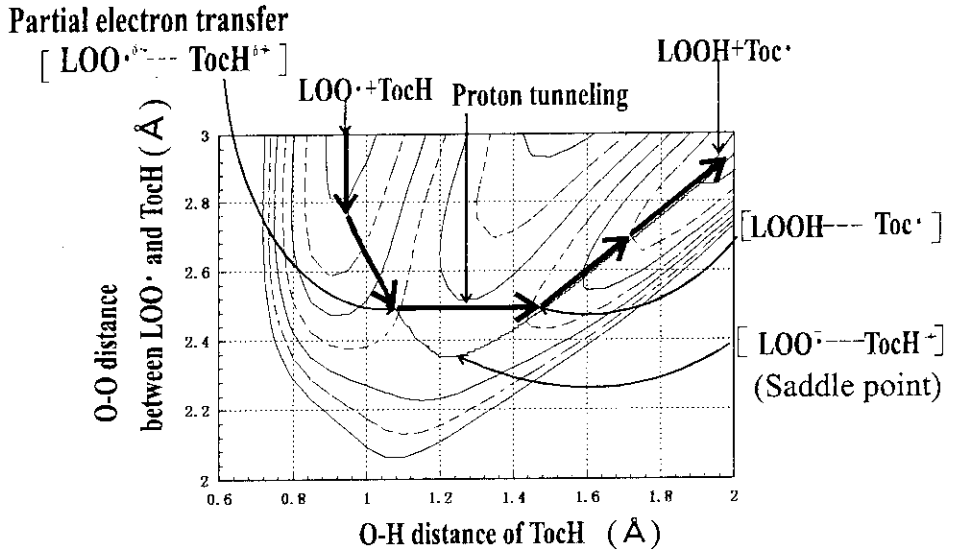

Figure 6. Calculated contour map of the potential surface in a model reaction for reaction 1. In the calculation, phenol and CH_3OO· were used instead of TocH and LOO·, respectively. The calculation method was AM1.

Prooxidant Reaction

In the description of a previous section, vitamin E is always advantageous *in vivo*. However, even oxygen, which is essential to life, produces a side effect and shortens the lifetime as mentioned above. Vitamin E should produce a side effect much more. The side effect is called the prooxidant reaction of vitamin E.

Figure 2 also shows the scheme of the prooxidant reaction of vitamin E (TocH).[15-18] Toc· participates in the prooxidant effect through the following reactions.

$$\text{Toc}\cdot + \text{LOOH} \rightarrow \text{TocH} + \text{LOO}\cdot \quad (5)$$

$$\text{Toc}\cdot + \text{LH} \rightarrow \text{TocH} + \text{L}\cdot \quad (6)$$

where reaction 5 is a reversal of reaction 1. Reaction 6 is a chain-transfer reaction and L· thus produced reacts with oxygen soon to produce LOO·, which accelerates lipid peroxidation together with LOO· produced from reaction 5. Reactions 5 and 6 are proton or hydrogen transfer reactions. We have performed the kinetic study of reaction 5 and have examined the role of proton tunneling in the prooxidant reaction of vitamin E.

In the present study, we have used stable 5,7-diisopropyl-Toc· and alkylhydroperoxide's (ROOH's) as models for Toc· and LOOH, respectively.

$$\text{Toc}\cdot + \text{ROOH} \xrightarrow{k_{-5}} \text{TocH} + \text{ROO}\cdot \quad (7)$$

The kinetic data of reaction 7 were obtained with a Shimadzu UV-2100S spectrophotometer

by mixing equal volume of solutions of 5,7-diisopropyl-Toc· and ROOH. The experimental procedures for the measurements of the second-order rate constants (k_{-s}'s) were described in detail elsewhere.[19]

Figure 7 shows a plot of $\log k_{-s}$ at 25 ℃ vs the Taft's σ^* constant of the alkyl substituents of ROOH studied.[20] k_{-s} increases, as σ^* decreases and the electron-donating capacity of ROOH increases. The plot in Figure 7 is found to be linear. These facts indicate that the charge transfer also plays an important role in reaction 5. Figure 7 also shows a plot of $\log k_{-s}$ for the reaction of deuterated ROOH (ROOD) and Toc· vs σ^*.

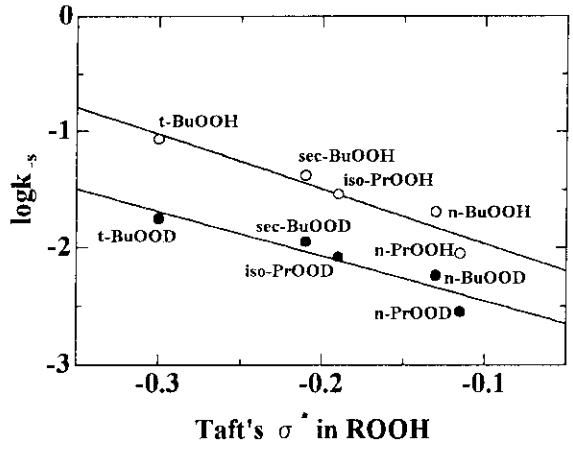

Figure 7. Plot of $\log k_{-s}$ in mixed solvent (benzene:ethanol=20:1) at 25 ℃ vs σ^* of the alkyl substituents of ROOH studied.

TABLE II: k_{-s}^H/k_{-s}^D at 25℃, E_{-act} and $\log A_{-s}$ for reaction 7 in mixed solvent (benzene : ethanol = 20 : 1), and σ^* of ROOH.

	k_{-s}^H/k_{-s}^D	E_{-act} (kJ/mol)	$\log A_{-s}$	σ^*
t－BuOOH	4.81	44.8±2.0	6.8±0.4	-0.300
t－BuOOD		52.7±2.0	7.5±0.3	
sec－BuOOH	3.72	55.6±0.5	8.4±0.1	-0.210
sec－BuOOD		58.2±3.2	8.3±0.6	
n－BuOOH	3.61	80.3±7.0	12.4±1.3	-0.130
n－BuOOD		86.2±6.0	12.9±0.9	
iso－PrOOH	3.46	71.1±3.1	10.9±0.6	-0.190
iso－PrOOD		73.2±1.9	10.8±0.3	
n－PrOOH	3.21	86.2±5.3	13.1±0.9	-0.115
n－PrOOD		87.0±3.8	12.6±0.7	

Table II shows the ratio of k_{-s} for ROOH to that of ROOD (k_{-s}^H/k_{-s}^D) at 25 ℃, the activation energy (E_{-act}) obtained from k_{-s} at 15-35 ℃, and the frequency factor (A_{-s}).

k_{-s}^{H}/k_{-s}^{D}'s of all the ROOH's do not exceed the maximum semi-classical isotope effect (13).[13] The difference in E_{-act} between ROOH and the corresponding ROOD does not exceed the maximum difference in zero-point energy (6.29 kJ/mol), either.[13] The ratio of A_{-s} for ROOH to that of ROOD also lies between 0.7 and 1.2 (criteria for semi-classical motion).[13] From these results, it is considered that proton tunneling does not play an important role in reaction 5.

Conclusions and Future Directions

The kinetic studies of the antioxidant and prooxidant reactions (reactions 1 and 5, respectively) of vitamin E have been carried out. The tunneling effect plays an important role in the antioxidant reaction, but not in the prooxidant reaction. Vitamin E is considered to inhibit the autoxidation of lipids in cellular membranes by taking advantage of the proton tunneling.

At present, we cannot unambiguously explain the reason for the presence and absence of the proton tunneling in the antioxidant and prooxidant reactions, respectively. However, it would be related to the fact that reactions 1 and 5 are exothermic and endothermic, respectively (see Tables I-II and Figure 8).

It would be very desirable at this point to obtain k_s's in the wider temperature range, which clarify the tunneling effect in reaction 1. It would also be worthwhile to study the role of tunneling in reaction 6 and the regeneration reaction of TocH by vitamin C. The calculation of the trajectory on the potential surface available for reactions 1 and 5 is also interesting.

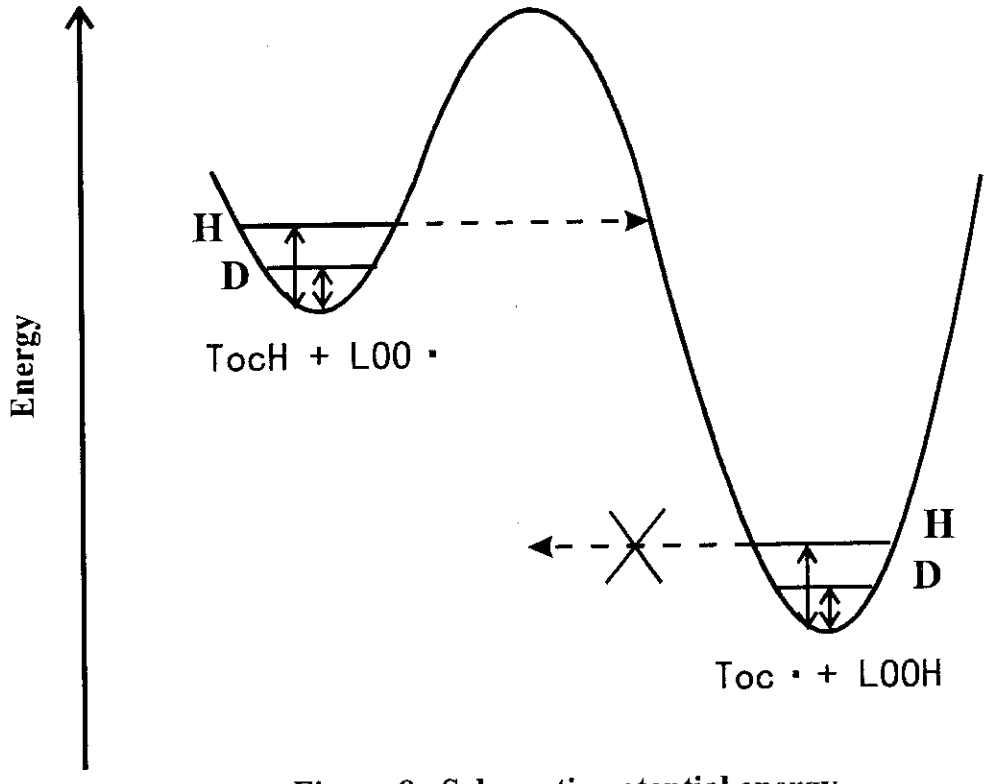

Figure 8. Schematic potential energy curve of reaction 1 and 5.

Most of experimental information regarding the proton (or hydrogen) transfer comes from observation in which either the appearance of proton-transferred species or the disappearance of the precursor of the proton transfer is measured. The researchers talk as if they could understand the whole story of 'Hamlet' from the first and last scenes alone. However, recently, reactions can be probed during the reaction process by means of the femtosecond spectroscopy.[21] Observations on the proton transfer during transfer have the possibility of giving new insight into chemical reactions.

Acknowledgment

We thank Eisai Co. Ltd. for the generous gift of *d*-α-, *d*-β-, *d*-γ-, and *d*-δ-TocH's. Our thanks are also due to the Computer Center of the Institute for Molecular Science for the use of the IBM SP2, NEC SX-3/34R, and HSP computers and the Library Program MOPAC.[22] This work was partly supported by a Grant-in-Aid for Scientific Research on Priority Area 'Quantum Tunneling of Group of Atoms as Systems with many Degrees of Freedom' (Area No. 271/08240231) from the Ministry of Education, Science, Sports and Culture of Japan. At last but not least, S.N. is deeply grateful to Professor Tetsuo Miyazaki of Nagaya University for his kind invitation to present a paper in the Meeting on Tunneling Reaction and Low Temperature Chemistry, 96 August.

References

[1]Cutler, R. G. *Free Radicals in Biology VI*; Pryor, W. A., Ed.; Academic Press: Orland, 1984; pp. 371-428.

[2]Burton, G. W.; Ingold, K. U. *Acc. Chem. Res.* **1986**, *19*, 194.

[3]Niki, E. *Chem. Phys. Lipids* **1987**, *44*, 227.

[4]Niki, E. *Yuki Gosei Kagaku* **1989**, *47*, 902.

[5]Kayden, H. J.; Traber, M. G. *J. Lipid Res.* **1993**, *34*, 343.

[6]Kuranaka, A.; Sawada, K.; Nagashima, U.; Nagaoka, S.; Mukai, K. *Vitamins* **1991**, *65*, 453.

[7]Nagaoka, S.; Kuranaka, A.; Tsuboi, H.; Nagashima, U.; Mukai, K. *J. Phys. Chem.* **1992**, *96*, 2754.

[8]Nagaoka, S.; Mukai, K.; Itoh, T.; Katsumata, S. *J. Phys. Chem.* **1992**, *96*, 8184.

[9]Nagaoka, S.; Inoue, M.; Miyazaki, T.; Mukai, K.; Nagashima, U. *Vitamin E Kenkyu no Shinpo V*; Vitamin E Kenkyu-kai Ed.; Kyoritsu Syuppan: Tokyo, 1995; pp. 56-62.

[10]Nagaoka, S.; Ishihara, K. *J. Am. Chem. Soc.*, **1996**, *118*,7361.

[11]Nagaoka, S. *Vitamins*, in press.

[12]Atkins, P. W. *Physical Chemistry* Fifth Edition; Freeman: New York, 1994; p. 864.

[13]Bell, R. P. *The Tunnel Effect in Chemistry*; Chapman and Hall: London, 1980; Chapter 4.

[14]Dewar, M. J. S.; Zoebich, E. G.; Healy, E.; Stewart, J. J. P. *J. Am. Chem. Soc.* **1985**, *107*, 3902.

[15]Cillard, J.; Cillard, P.; Cormier, M.; Girre, L. *J. Am. Oil Chem. Soc.* **1980**, *57*, 252.

[16]Peers, K. E.; Coxon, D. T.; Chan, H. W-S. *J. Sci. Food Agric.* **1981**, *32*, 898.

[17]Terao, J.; Matsushita, S. *Lipids* **1986**, *21*, 255.

[18]Nagaoka, S.; Okauchi, Y.; Urano, S.; Nagashima, U.; Mukai, K. *J. Am. Chem. Soc.* **1990**,

112, 8921.
[19]Nagaoka, S.; Sawada, K.; Fukumoto, Y.; Nagashima, U.; Katsumata, S.; Mukai, K. *J. Phys. Chem.* **1992**, *96*, 6663.
[20]Taft Jr., R. W. *Steric Effects in Organic Chemistry*; Newman, M. S. Ed.; Wiley: New York, 1956; Chapter 13.
[21]Zewail, A. H.; Bernstein, R. B. *C&EN* **1988**, 24.
[22]Stewart, J. J. P. *QCPE No. 455*, 1983.

9. Reaction of Long-lived Radicals and Vitamin C in γ-Irradiated Mammalian Cells and Their Model System at 295 K. Tunneling Reaction in Biological System

TAKURO MATSUMOTO,[1] TETSUO MIYAZAKI,[1,2] YOSHIO KOSUGI,[3] TAKAYUKI KUMADA,[2] SINJI KOYAMA,[4] SEIJI KODAMA[4] and MASAMI WATANABE,[4]

[1]Department of Applied Chemistry, School of Engineering, Nagoya University, Furo-cho, Chikusa-ku, Nagoya 464-01, [2]Advanced Science Research Center, Japan Atomic Energy Research Institute, Tokai-mura, Ibaraki 319-11, [3]Department of Material Science, The Faculty of Science & Technology, Shimane University, Matsue 690 and [4]Division of Radiation and Life Science, Faculty of Pharmaceutical Sciences, Nagasaki University, 1-14 Bunkyo-cho, Nagasaki 852, Japan

Abstract — When golden hamster embryo (GHE) cells or concentrated albumin solution (0.1 kg dm^{-3}) that is a model system of cells is irradiated with γ-rays at 295 K, organic radicals produced can be observed by ESR. The organic radicals survive at both 295 K and 310 K for such a long time as 20 hr. The long-lived radicals in GHE cells and the albumin solution react with vitamin C by the rate constants of 0.007 dm^3 mol^{-1} s^{-1} and 0.014 dm^3 mol^{-1} s^{-1}, respectively. The long-lived radicals in human cells cause gene mutation, which is suppressed by addition of vitamin C. The isotope effect on the rate constant (k) for the reaction of the long-lived radicals and vitamin C has been studied in the albumin solution by use of protonated vitamin C and deuterated vitamin C. The isotope effect (k_H/k_D) was more than 20∼50 and was interpreted in terms of tunneling reaction.

It has been suggested that vitamin C is effective for suppression of some kinds of cancer (Dunham et al., 1982). The mechanism for the suppression of cancer may be related to the scavenging activity of vitamin C, which is a well-known radical scavenger in biological systems. The rate constants for the reaction of vitamin C with radicals have been reported previously in a dilute aqueous solution (Ohno, 1991; Parker, 1980).

When golden hamster embryo (GHE) cells or the aqueous albumin solution (0.1 kg dm^{-3}) is irradiated with γ-rays at 295 K, organic radicals produced survive for more than 24 hr at room temperature (Yoshimura et al., 1993). Very recently we have found that vitamin C reacts with the long-lived organic radicals in the γ-irradiated albumin solution at high concentration of 0.1 kg dm^{-3} by the rate constant of 0.014 dm^3 mol^{-1} s^{-1}(Miyazaki et al., 1995), which is much smaller than the reported rate constants (10^6 − 10^{10} dm^3 mol^{-1} s^{-1}) for the reaction of vitamin C with radicals in a dilute aqueous solution .

Here we have undertaken to solve the following three problems . The first problem is to measure the rate constant for the reaction of vitamin C with long-lived radicals in γ-irradiated GHE cells. Does the rate constant in the GHE cells coincide with that in the concentrated protein solution or with that in the dilute aqueous solution ?

The second problem is whether or not the reaction of vitamin C with the long-lived radicals in GHE cells is related to biological effects in the irradiated cells. It is important to examine the correlation between chemical reactions in biological systems and biological effects.

The third problem is whether or not the reaction of vitamin C with the long-lived radical is caused by a quantum-mechanical tunneling effect. It is confirmed that a hydrogen-atom-transfer reaction in solid hydrogen at very low temperature takes place by tunneling (Miyazaki et al., 1992). Since most of reactions in biological systems including the reaction of vitamin C are a transfer of a hydrogen atom or a proton that has a large wave character, it is generally expected that the tunneling reaction may play an important role in biological systems at room temperature. The studies of isotope effects on reactions will give an information on the contribution of tunneling reaction.

EXPERIMENTAL

GHE cells were obtained from 13- to 14-day-old embryos. Tissues from a litter of embryos, exclusive of crania and bowels, were pooled and minced with scissors and trypsinized with 0.0025 kg dm^{-3} trypsin solution at 310 K for 20 min to make a cell suspension. Cells were washed four times with phosphate-buffered-saline and centrifuged to avoid contamination of serum and trypsin. For mutation experiments, we used primary human embryo (HE) cells which were grown in Eagle's MEM supplemented with 0.2 mM serum, 0.2 mM aspartate, 1.9 mM pyruvate and 10 % fetal bovine serum. 10^6 cells were inoculated into 25 cm^2 culture bottles and incubated at 37 °C for 6 days. Then, the confluent cells were used for mutation experiments. Cells were treated with 0.001 kg dm^{-3} of vitamin C at 20 min or 20 hr at 310 K after x-irradiation at 295 K. After treatment for 2 hr, cells were harvested by trypsinization for mutation assay. An aqueous solution of protein (albumin, egg) at 0.1 kg dm^{-3} was used as a model of cells. The purity of vitamin C (*h*-vitamin C) was greater than 99 mol%. Deuterated vitamin C (*d*-vitamin C) was obtained by dissolving *h*-vitamin C in deuterated water and then drying the solution in a vacuum line. NMR analysis of the prepared *d*-vitamin C indicated that two OH groups connected to a double bond were changed into OD groups.

Samples were irradiated with γ-rays from a ^{60}Co source at 295 K. The ESR spectra of radicals were obtained using a JES-FE2XG ESR spectrometer (JEOL) at 77 K. The yields of radicals were obtained by double integration of the spectra.

For mutation assay, sufficient numbers of target cells were irradiated to insure at least 10^6 survivors. The cells were grown for 14 days after x-rays irradiation for mutation expression, then trypsinized, resuspended into a medium containing 40 μ M 6-thioguanine and plated onto plastic dishes (64 cm^2) at 7.8×10^2 cells per cm^2. The cells were incubated in a 5 % CO_2 incubator for 16 days. The frequency of mutants was expressed as the ratio of the number of mutants to 10^6 survivors.

RESULTS

When GHE cells or albumin solution (0.1 kg dm^{-3}) is irradiated with γ-rays at 295 K, organic radicals produced can be observed by ESR and their ESR spectra were reported in the previous paper (Yoshimura et al., 1993). Figure 1 shows the yields of organic radicals, produced by γ-irradiation at 295 K and stored at 295 K or 310 K. The yields of radicals in GHE cells decay fast in several hours and become nearly constant from 3 hr to 20 hr, indicating the presence of long-lived radicals. The decay behavior of the radicals in GHE cells at 295 K are approximately similar to that at 310 K. The decay rate of albumin radicals in H_2O-albumin(0.1 kg dm^{-3}) is the same as that in D_2O-albumin(0.1 kg dm^{-3}), indicating that there is no isotope effect on the decay rates of long-lived radicals. Since the decay behavior of albumin radicals in the aqueous albumin solution is approximately similar to that of organic radicals in the GHE cells, the concentrated albumin solution can be used for study of the long-lived radicals as a model system of GHE cells.

Figure 2 shows the effect of vitamin C on the yields of organic radicals in γ-irradiated GHE cells stored at 295 K. Vitamin C at 0.008 kg dm^{-3} or 0.02 kg dm^{-3} was added at 2 hr after γ-irradiation. The radicals in the γ-irradiated GHE cells decay fast upon addition of vitamin C, while they decay very slowly in the absence of vitamin C.

Figure 3 shows the effect of vitamin C on the yields of albumin radicals in γ-irradiated H_2O-albumin solution (0.1 kg dm^{-3}) stored at 295 K. Vitamin C at 0.002 kg dm^{-3} was added at 2 hr after γ-irradiation. The radicals in the γ-irradiated H_2O-albumin solution decay fast upon addition of vitamin C, while they decay very slowly in the absence of vitamin C.

Figure 4 shows the effect of deuterated vitamin C (*d*-vitamin C) on the yields of albumin radicals in γ-irradiated D_2O-albumin solution (0.1 kg dm^{-3}) stored at 295 K. *d*-Vitamin C at 0.002 kg dm^{-3} was added at 2 hr after γ-irradiation. The radicals in the γ-irradiated D_2O-albumin solution decay slowly in the presence of *d*-vitamin C as well as in the absence of it.

Figure 5 shows the effect of vitamin C on mutation frequency at hypoxanthin guanine phosphoribosyltransferase gene locus of human

embryo (HE) cells irradiated with x-rays. The mutation frequency was represented against doses of the irradiation. It is pointed out that the mutation frequencies produced in the irradiated HE cells are approximately similar to those in GHE cells (Watanabe and Suzuki, 1991). The mutation frequency in HE cells were reinoculated for mutation assay at 20 min or at 20 hr after irradiation without vitamin C treatment. Vitamin C at 0.001 kg dm^{-3} was added at 20 min after the irradiation or at 20 hr after the irradiation. The cells were treated with vitamin C for 2 hr, and then reinoculated for mutation assay. The mutation frequency in the absence of vitamin C increases with the increase of the irradiation-dose. When vitamin C was added after the irradiation, the mutation frequency was suppressed completely.

DISCUSSIONS

Reaction of Long-lived Radicals and Vitamin C

Figure 1 shows clearly that organic radicals produced by γ-irradiation of GHE cells and a concentrated albumin solution survive at 295 K for such a long time as 20 hr. When vitamin C is added to the irradiated samples, the radicals decay fast by a reaction with vitamin C (cf. Figures 2 and 3).

$$\text{cells (or albumin solution)} \xrightarrow{\wedge\!\!\wedge} \text{R}\cdot \qquad (1)$$

$$\text{R}\cdot + \text{vitamin C} \longrightarrow \text{P} \qquad (2)$$

where R · represents long-lived radicals produced by the γ-irradiation of the cells or the albumin solution. Reaction (2) is a hydrogen-atom (or a proton) transfer reaction from vitamin C to the long-lived radicals, where P is some products (Bielski, 1982). The rate constant for reaction (2) was estimated as 0.007 $dm^3\ mol^{-3}\ s^{-1}$ from the results in Figures 2 and 3, by assuming a pseudo-first-order reaction, since the concentration of vitamin C is much larger than that of long-lived radicals.

Though the rate constant (0.007 $dm^3\ mol^{-1}\ s^{-1}$) for the reaction with long-lived radicals in GHE cells is roughly the same order of magnitude as that (0.014 $dm^3\ mol^{-1}\ s^{-1}$) in a concentrated albumin solution, it is much smaller than those (10^6 — 10^{10} $dm^3\ mol^{-1}\ s^{-1}$) for the reaction in a dilute aqueous solution. The reactions in the cells take place in polymer coils,

where the diffusion of reactants is strongly restricted, resulting in a small rate constant. Since the rate constant in GHE cells are approximately similar to that in the concentrated albumin solution, the concentrated albumin solution can be used as a model of GHE cells for study of the reaction of vitamin C and long-lived radicals.

Biological Effects of Long-lived Radicals in γ-Irradiated Human Embryo Cells

Since the mutation frequency in HE cells increases approximately linearly with the increase of irradiation doses, the mutation is caused by the reactive species produced by the irradiation (cf. Figure 5). The mutation frequency is suppressed drastically upon addition of vitamin C after the irradiation(cf. open triangles in Figure 5). Even if vitamin C is added at 20 hr after the irradiation, the mutation is suppressed effectively (cf. closed triangles in Figure 5). Thus, the reactive species that are responsible for the mutation have a long lifetime.

$$\text{cells} \xrightarrow{\wedge\wedge} \text{R}\cdot \qquad (1)$$

$$\text{R}\cdot \longrightarrow \text{gene mutation} \qquad (3)$$

$$\text{R}\cdot + \text{vitamin C} \longrightarrow \text{P} \qquad (2)$$

Because vitamin C can completely restrain mutation induced by x-rays, the long-lived radicals (R・) are regarded as a cause of mutation. The long-lived radicals that are produced probably in lipids or proteins of cells may disturb some kinds of biological reactions in cells and may relate finally to the mutation.

Isotope Effects on Reaction of Long-lived Radicals and Vitamin C

The isotope effect on the reaction of long-lived radicals and vitamin C has been studied by use of protonated vitamin C (*h*-vitamin C) in H_2O-albumin solution and deuterated vitamin C (*d*-vitamin C) in D_2O-albumin solution, which can be considered as a model of cells for the study of the reaction of vitamin C. Figure 3 shows clearly that *h*-vitamin C reacts effectively with long-lived albumin radicals. When *d*-vitamin C is added to

the irradiated D_2O-albumin solution, however, albumin radicals decay only slightly faster than those in the absence of *d*-vitamin C, indicating that *d*-vitamin C does not react with the radicals so effectively as *h*-vitamin C does (cf. Figure 4). Then, we can estimate roughly the isotope effect (k_H/k_D) on the following reactions.

$$R\cdot + \textit{h}\text{-vitamin C} \longrightarrow RH + \textit{h}\text{-vitamin C}\cdot \quad (4)$$

$$R\cdot + \textit{d}\text{-vitamin C} \longrightarrow RD + \textit{d}\text{-vitamin C}\cdot \quad (5)$$

k_H and k_D are the rate constants for reactions (4) and (5), respectively. *h*-Vitamin C· and *d*-vitamin C· are the radicals produced from vitamin C by the hydrogen-atom (or proton)-transfer reaction. Since the vitamin C· radicals can diffuse fast in the solution, they disappear and cannot be observed by ESR. The isotope effect (k_H/k_D) was estimated as $\geqq 20\sim 50$ by comparing the decay rates of albumin radicals in Figure 3 with those in Figure 4.

Now, we will discuss the large isotope effect on the reaction by a simple theoretical treatment. The difference in the activation energies for reactions (4) and (5) , i. e., $E_d - E_h$, is assumed here to be less than 1 kcal mol^{-1}, which is caused probably by the difference in zero-point-vibration energies of *h*-vitamin C, *d*-vitamin C, and an activated complex for the reaction (Bell, 1980) . If the reaction takes place by passing over the potential barrier for the reaction, the isotope effect for the reaction is expected as less than 6, which is much smaller than the experimental value ($\geqq 20\sim 50$) for the reaction (cf. Table 1). Though the potential energy curves for the reactions (4) and (5) are unknown, the curves are approximated to two types of a potential barrier: a parabolic barrier (a barrier height (E_h) for reaction (4), 10～15 kcal mol^{-1}; $E_d - E_h$, 1 kcal mol^{-1}; a width at half height of the barrier, 0.06～0.07 nm) and a Eckart barrier (a barrier height for reaction (4), 11～14 kcal mol^{-1}; $E_d - E_h$, 1 kcal mol^{-1}; a width at half height of the barrier, 0.07～0.09 nm). If the reaction takes place by passing through the barrier by a tunneling effect, we can calculate the rate constant for the tunneling reaction (Bell, 1980). The isotope effects are expected as 20～70 for the parabolic barrier and 20～60 for the Eckart barrier, which are roughly similar to the experimental value ($\geqq 20\sim 50$) for the isotope effect on the reaction (cf. Table 1). Therefore, it is concluded that the reaction of long-lived radicals and vitamin C takes place by a tunneling effect. It is well-known that the multiplication of cells is

suppressed drastically by addition of D_2O (Tanaka et al., 1994). The suppression may be related to a large isotope effect on biological processes, caused probably by a tunneling reaction.

Acknowledgment — This work was supported by a Grant for Scientific Research from the Japanese Ministry of Education, Science and Culture, and by a Grant for the Regional Links Research Program at Nagasaki of the Research Development Corporation of Japan.

REFERENCES

Bell R. P. (1980) *The Tunnel Effect in Chemistry*, Chapman and Hall, London.

Bielski B. H. J. (1982) *Advances in Chem. Series* **200**, 81.

Dunham W. B., Zuckerhandl E., Reynolds R., Willoughby R., Marcuson R., Barth R. and Pauling L. (1982) *Proc. Natl Acad. Sci. U. S. A.* **79**, 7532.

Miyazaki T., Kitamura S., Morikita H. and Fueki K. (1992) *J. Phys. Chem.* **96**, 10331, and related papers cited therein.

Miyazaki T., Yoshimura T., Mita K., Suzuki K. and Watanabe M. (1995) *Radiat. Phys. Chem.* **45**, 199.

Ohno S.(1991) *Handbook of Radiation Chemistry* (Edited by Tabata Y., Ito Y. and Tagawa S.) p. 321, CRC Press, Boston.

Parker J. E., Willson P. L., Bahnemann D. and Asmus K. (1980) *J. Chem. Soc., Perkin Trans.* **2**, 296.

Tanaka T., Udagawa J. and Hatta T. (1994) *Chemistry and Chemical Industry,* 47, 224 (in Japanese).

Watanabe M. and Suzuki K. (1991) *Mutation Res.* **249**, 71.

Yoshimura T., Matsuno K., Miyazaki T., Suzuki K. and Watanabe M. (1993) *Radiat. Res.* **136**, 361.

Table 1. Isotope Effect on Rate Constants for Reactions of *h*-Vitamin C and *d*-Vitamin C

	k(*h*-vitamin C) / k(*d*-vitamin C)
experimental reaction	≧ 20～50
classical reaction [a]	≦ 6
tunneling reaction 1 [b]	20～70
tunneling reaction 2 [c]	20～60

[a] The value estimated by the model that the difference between in the activation energies for the reactions of *h*-vitamin C and those of *d*-vitamin C is less than 1 kcal mol^{-1}. [b] The value calculated by the model that the potential energy curve for the reaction is approximated to a parabolic barrier (see text). [c] The value calculated by the model that the potential energy curve for the reaction is approximated to a Eckart barrier (see text).

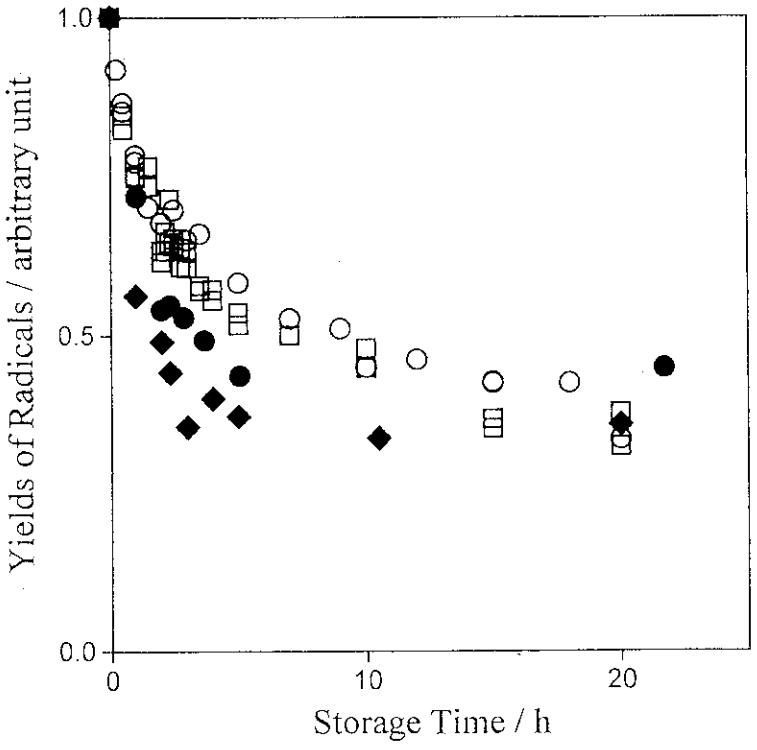

Fig. 1. Decay of organic radicals produced by γ-irradiation at 295 K with 5 kGy for GHE cells and with 4.3 kGy for albumin solution (0.1 kg dm^{-3}) : (●) GHE cells stored at 295 K; (◆) GHE cells stored at 310 K; (○) H_2O-albumin solution stored at 295 K ; (□) D_2O-albumin solution stored at 295 K.

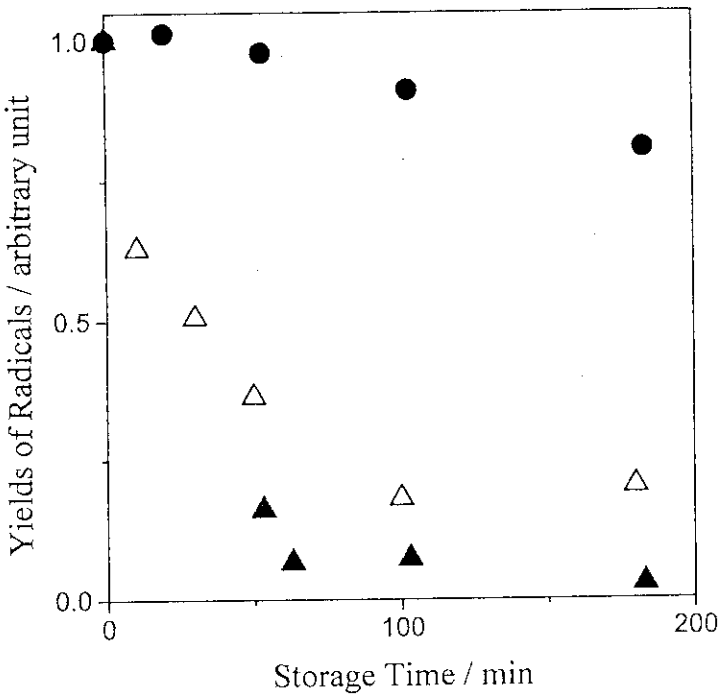

Fig. 2. Effect of vitamin C on the yields of organic radicals in GHE cells γ-irradiated with 5 kGy and stored at 295 K. Vitamin C was added at 2 hr after the irradiation and then the yields of the radicals were measured: (●) GHE; (△) GHE-vitamin C(0.008 kg dm^{-3}); (▲) GHE-vitamin C(0.02 kg dm^{-3}).

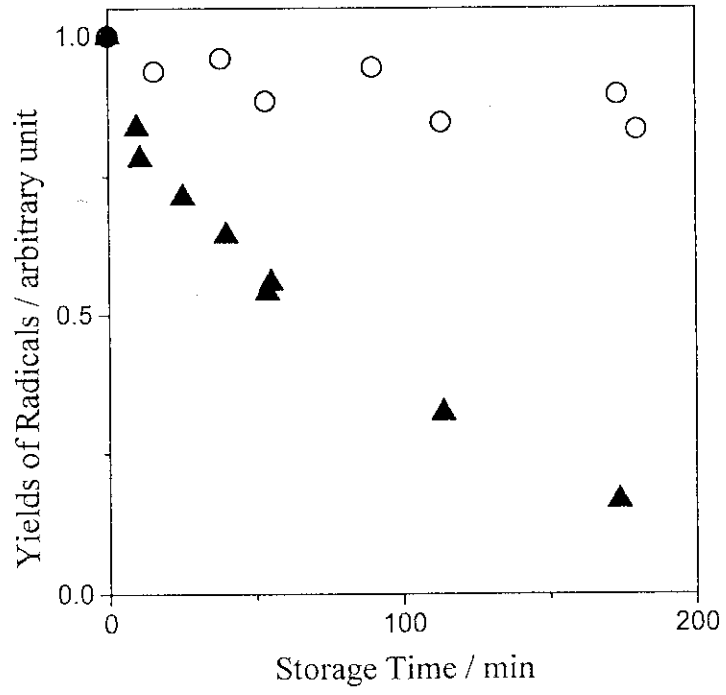

Fig. 3. Effect of vitamin C on the yields of albumin radicals in H_2O-albumin solution (0.1 kg dm^{-3}) γ-irradiated with 4.3 kGy and stored at 295 K. Vitamin C(0.002 kg dm^{-3}) was added at 2 hr after the irradiation and then the yields of the radicals were measured: (○) H_2O-albumin; (▲) H_2O-albumin-vitamin C.

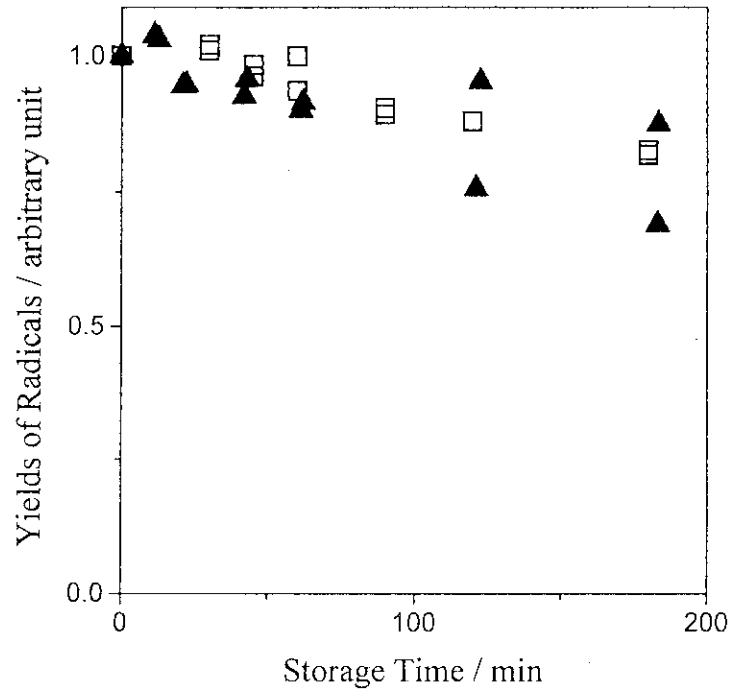

Fig. 4. Effect of *d*-vitamin C on the yields of albumin radicals in D_2O-albumin solution (0.1 kg dm^{-3}) γ-irradiated with 4.3 kGy and stored at 295 K. *d*-Vitamin C(0.002 kg dm^{-3}) was added at 2 hr after the irradiation and then the yields of the radicals were measured: (□) D_2O-albumin; (▲) D_2O-albumin-*d*-vitamin C.

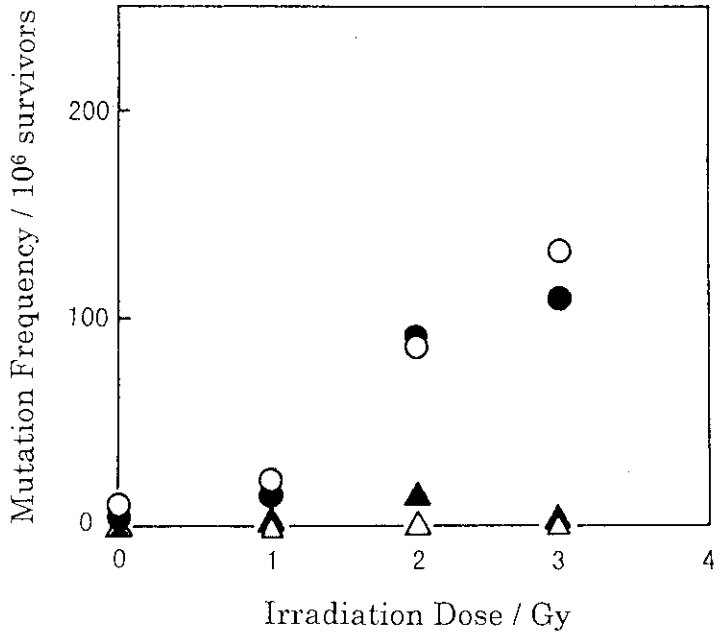

Fig. 5. Effect of vitamin C on gene mutation caused by x-rays irradiation of human embryo cells: (○) Cells were irradiated and reinoculated at 20 min after irradiation for mutation assay; (●) Cells were irradiated and reinoculated at 20 hr after irradiation for mutation assay; Cells were treated with 0.001 kg dm^{-3} of vitamin C for 2 hr at 20 min (△) or 20 hr (▲) after irradiation and, then reinoculated for mutation assay.

10. Biological Effects of Radiation−indeced Long Life Radical in Mammalian Cells and Effective Scavenging It by Vitamin C

Masami Watanabe, Shinji Koyama, Keiji Suzuki, Seiji Kodama, Takurou Matsumoto[1)], and Tetsuo Miyazaki[1)]

Laboratory of Radiation and Life Science, School of Pharmaceutical Sciences, Department of Health Sciences, Nagasaki University, Nagasaki 852, Japan and [1)]Nagoya University, Nagoya 500, Japan

Many researcher studying in area of radiation biology have been believed that active short life-time radicals such as OH and H radicals, play an important role to express biological effects of radiations in cells, such as cell killing and mutation induction. However, we recently found a new type of radicals with long life-time in cells(T1/2>20hr) using electron spin resonance(ESR) method and it may be more important in mutation induction than the active short-live radicals. When cells were treated with radical scavengers such as DMSO and vitamin C just before irradiation, short life-time radicals were scavenged well. However, if cells were treated with scavengers after irradiation, vitamin C scavenge the long life-time radicals well, but DMSO did not. In addition, vitamin C treatment after irradiation drastically reduced mutation frequency at *hprt* locus in human cells and morphological transformation in Syrian hamster cells, but DMSO treatment did not. These results suggested that mutation is probably caused by the presence of radicals with a long lifetime in the cells, rather than short life-time radicals. Vitamin C reacts with long life-time radicals efficiently, resulting in the decrease of the mutation induction.

Although we could not answered the question that what is the main body of this radical now, but we expected that is a kind of hyperoxidated organic radical because ESR spectrum showed a typical asymmetric structure of it. This thing suggests the possibility that the cell damage to cause mutation and transformation produces through active oxygen. So we examined whether mutation frequency in mammalian cells was influenced by existence of oxygen. As a result, I understood that mutation frequency in cells cultured under nitrogen condition was reduced to the almost half of that in cells under oxygen condition. Induction of mutation after X-irradiation completely suppressed by treatment by vitamin C under nitrogen condition, too. Radio protective effects The influence of radical scavenger was not watched by nitrogen substitution for cell inactivation rate and chromosome aberration frequency .

In any case, we have to concluded that the initial lesion to produce mutation is different at all from those to produce chromosome aberration and cell inactivation.

Radical of high reactivity participates in the creation of damages (such as chromosome aberration) to cause cell death. Organic radical of longevity life participates in the creation of damages (such as mutational and transform- ational damages) that is not related to life and death of a cell . From a result provided by this study, we suggest the hypothesis that seems to be shown in figure 1. By X-radiation, two kind of radicals forms in mammalian cells at least.One is the short life radical

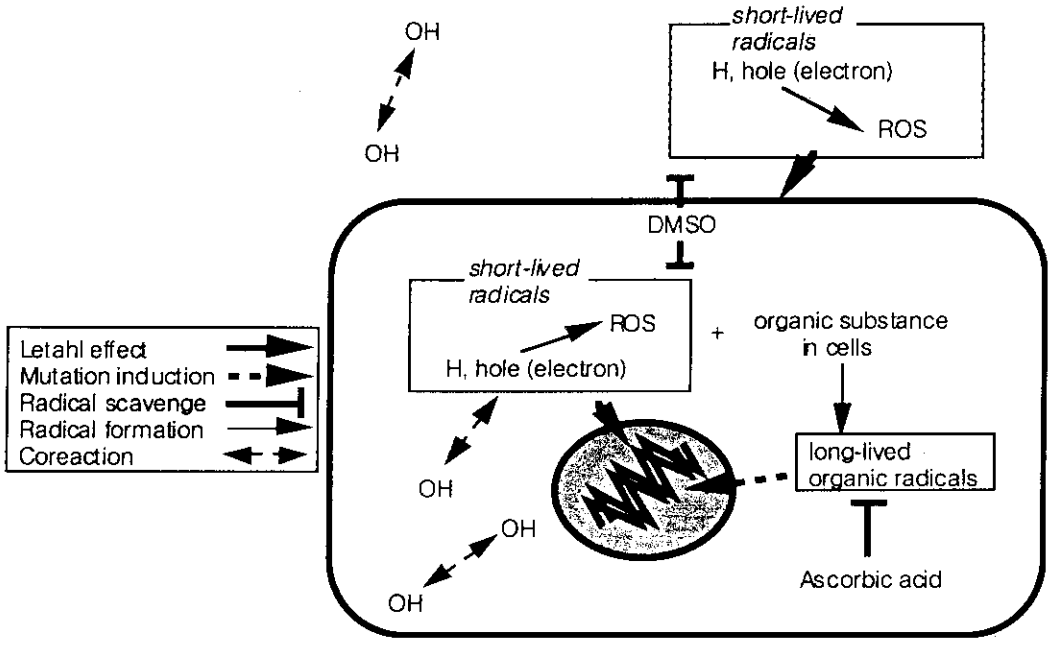

Figure 1 Expected reaction mechanisum of radiation- induced radicals in mammalian cells.

that activity is high and the other is the long life organic radical that activity is low. The former may produce many DNA strand breaks. If DNA breaks were not repaired well, it causes chromosome aberration, and cell death. The latter produces wound of small scale in DNA. Therefore, cells do not died for this lesions even if cells could not completely repair them. Wound of DNA left causes DNA reproduction abnormality, and they causes mutation. Because vitamin C specifically catches organic radical, frequency of mutation is decreased. If a serial hypothesis is right, this is expected when a change to be left with DNA of mutant cell occurring after vitamin C handling is the deficiency type which is large scale.

Reference

1.T.Miyazaki, Y.Hayakawa, K.Suzuki, M.Suzuki and M.Watanabe (1990) *Radiat. Res.*, 124 , 66-72.
2.M.Watanabe, M.Suzuki, K.Suzuki, Y.Hayakawa and T.Miyazaki (1990) *Radiat. Res.*, 124 , 73-78.
3.T.Yoshimura, T.Miyazaki, S.Mochizuki, K. Suzuki, and M. Watanabe (1992) *Radiat. Phys. Chem.*, 40 , 45-48 .
4.T.Miyazaki, T. Yoshimura, K.Mita, K.Suzuki., and M. Watanabe (1994) *Radiat. Phys. Chem.*, 45 , 199-202 (1994)
5.T.Miyazaki, T.Yoshimura, K.Suzuki, amd M.Watanabe (1994) *Magnetic Resonance in Med.*, 6, 346-348.

11. Radiation Sensitivities of *Escherichia coli* to Gamma-rays under Deep Frozen Conditions

Machiko Takigami and Hitoshi Ito
Department of Radiation Research for Environment and Resources, JAERI Takasaki

Introduction

Radiation damage on living organisms is induced by direct and indirect effects. Gamma-irradiation to living organisms in aqueous media is greatly effected by hydroxyl radicals produced by the radiolysis of water. However, radiation effect under frozen conditions is not clear. In order to know the effect of free radicals on microorganisms in aqueous media, gamma-irradiation was carried out under deep frozen conditions, because the movement of hydroxyl radicals is expected to be restricted under these conditions. Irradiation of *E. coli* was also carried out in the presence of glycerol, a kind of radical scavenger.

Experimental

Materials

Escherichia coli B1 isolated from *E. coli B* as a radiosensitive strain and *E. coli* B/r as a radiation resistant strain were used for the experiment. They were inoculated in nutrient broth and incubated for 16h at 30℃. The cells in stationary phase were collected by centrifugation and washed twice with phosphate buffer solution (0.067 M, pH 7.0). They were suspended in phosphate buffer solution so that the concentration was to be ca. 10^8 cells/ml and subjected for irradiation. Glycerol was added to the cell suspension in some experiments.

Irradiation

The cell suspensions under air equilibrium were irradiated with ^{60}Co gamma-rays at the dose rate of 1.2 kGy/h at room temperature, dry-ice-methanol temperature (ca. -70℃) and liquid nitrogen temperature (-196℃). The dose rate was determined by Fricke's dosimetry.

Plating

The irradiated samples were diluted with 0.85% saline solution with 0.01% Tween 20 (polyoxyethylene (20) sorbitan monolaurate) and plated on MacConkey agar plates. The plates were incubated at 37℃ until the colonies were formed. Counting the colonies, survival fractions were obtained as Ni/Nc, where Ni and Nc stand for the number of colonies in the irradiated sample and control sample, respectively.

Results and Discussion

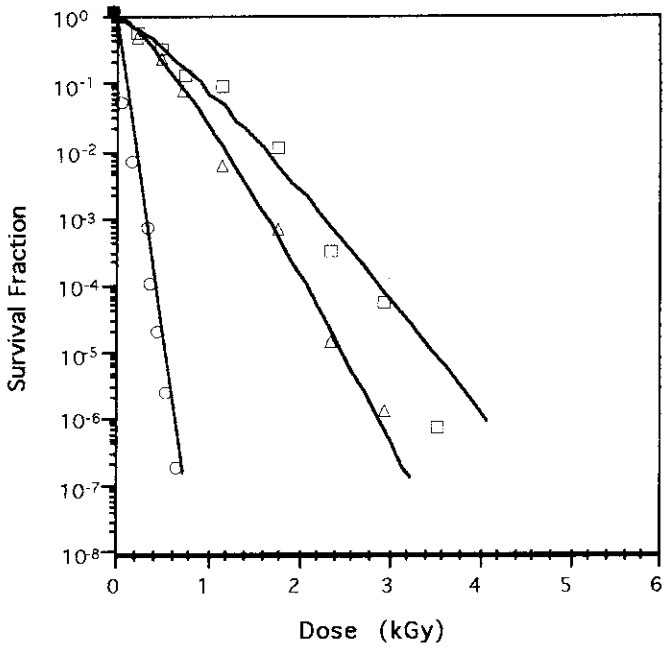

Figure 1 Survival curves of gamma-irradiated *E. coli* B1 suspended in phosphate buffer solution. Irradiation at : (○) : room temperature, (△): dry-ice-methanol temperature, and (□): liquid nitrogen temperature.

The survival curves of *E. coli* B1 irradiated under various conditions are shown in Figure 1. Although *E. coli* B1 is a radiosensitive strain and does not show a shoulder when irradiated in the phosphate buffer solution at room temperature, it becomes radioresistant and shows a shoulder when irradiated under deep frozen conditions. With the decrease of irradiation temperature under deep frozen conditions, the strain is more resistant to gamma-irradiation. The phenomena imply that radiation sensitivity of *E. coli* to gamma-rays under deep frozen conditions can not be elucidated only by direct effect.

In order to clarify the role of free radicals at low temperature, Fricke's dosimetry was carried out not only at room temperature but also under deep frozen conditions. The Fricke's solution was irradiated at 10cm distance from the radiation source. The absorbance at 304 nm is shown in Figure 2. The absorbance decreased with the decrease of irradiation temperature. The relative slope of each line was 1.0, 0.15 and 0.07 for irradiation at room temperature, -70℃ and -196℃, respectively. The results correspond to the radiosensitivity of *E. coli* B1 under deep frozen conditions. However, the radiosensitivity can not be explained only by the dose in appearance under deep frozen conditions. Under dissolved oxygen equilibrium, Fe^{2+} is oxidized to Fe^{3+} by the action of OH•, HO_2• and H_2O_2. All those radiolytic products come from water. Among those active species, it has been said that OH• is responsible for the indirect effect of radiation to living organisms. OH• is very mobile at room temperature, however, its movement is restricted at -196℃.

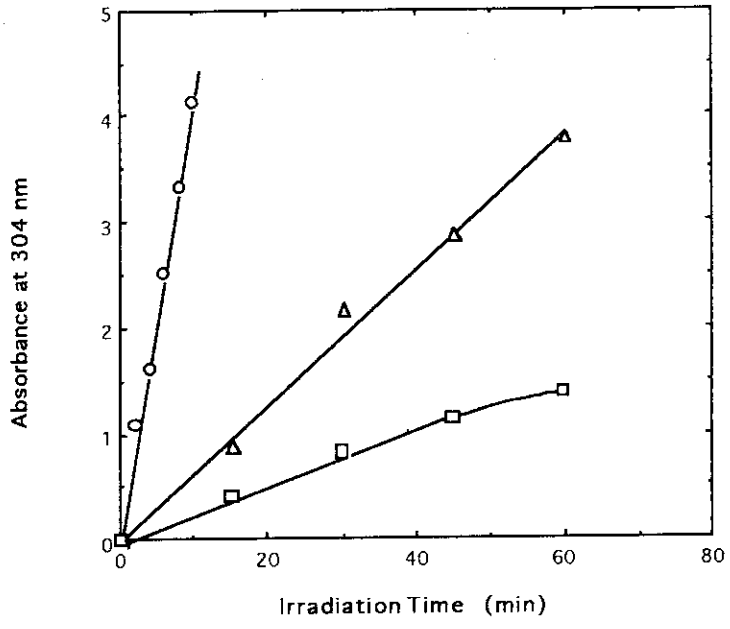

Figure 2 Fricke's dosimetry at various temperatures. Irradiation at : (○): room temperature, (△): dry-ice-methanol temperature, and (□) : liquid nitrogen temperature.

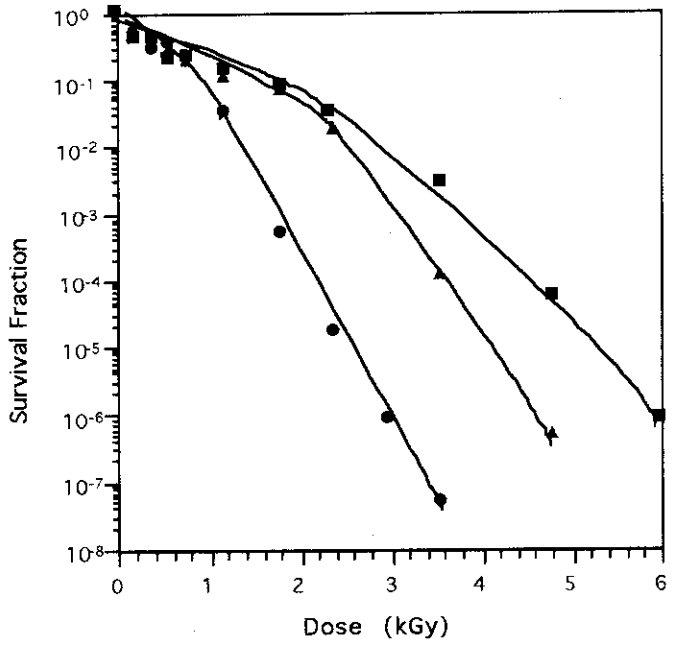

Figure 3 Survival curves of gamma-irradiated *E. coli* B1 suspended in phosphate buffer solution containing 5% glycerol. Irradiation at : (●): room temperature, (▲): dry-ice-methanol temperature, and (■): liquid nitrogen temperature.

In the presence of 5% glycerol, a radical scavenger, *E. coli* B1 was irradiated at various temperatures. The same tendency which was observed for the irradiation in phosphate buffer solution is observed as shown in Figure 3. When irradiated in the presence of glycerol, the strain is more resistant to radiation at room temperature and under deep frozen conditions.

The effects of glycerol concentration on survival of gamma-irradiated and UV-irradiated *E. coli* B1 are shown in Figures 4 and 5, respectively. With the increase of glycerol from 5 to 10%, radiation resistance is increased slightly in gamma-irradiated samples. Although glycerol shows a great effect on survival of gamma-irradiated *E. coli*, it shows little effect on UV-irradiated samples. Therefore, one of the roles of glycerol is to protect cells by scavenging radicals produced by gamma-irradiation.

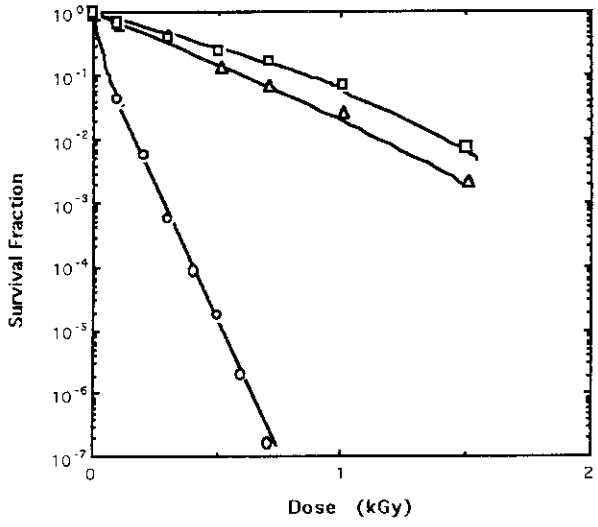

Figure 4 Effect of glycerol on survival of gamma-irradiated *E. coli* B1. Irradiated in : (○): phosphate buffer solution, (△): 5% glycerol and (□): 10% glycerol.

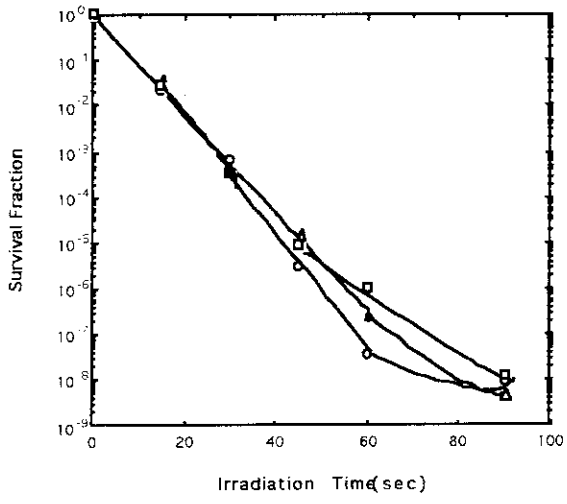

Figure 5 Effect of glycerol on survival of UV-irradiated *E. coli* B1. Irradiated in : (○): phosphate buffer solution, (△): 5% glycerol and (□): 10% glycerol.

E. coli B/r showed a similar tendency to *E. coli* B1 concerned with the effect of temperature and glycerol on survival fraction, as shown in Figure 6.

D_{10} values of *E. coli* B1 and B/r irradiated under various conditions are shown in Table 1. D_{10} values of the strains are increased with the decrease of temperature and by addition of glycerol to the suspension. The decrease of temperature restricts the movement of radicals and the addition of glycerol decreases the number of radicals by scavenging them. As the effect of temperature and glycerol on survival of gamma-irradiated *E. coli* is different among the strains, it is implied that the amount of some protective substance is different from the strains. The substance is considered to be rich in *E. coli* B1 and not rich in B/r.

Conclusions

It was clarified that the sensitivities of *E. coli* to gamma-irradiation were decreased with the decrease of temperature even under deep frozen conditions. The sensitivities were decreased drastically by the addition of glycerol, a radical scavenger, to the suspension of *E. coli*. The phenomena were elucidated as follows: the indirect effect of radiolytic products from water decreases with the decrease of irradiation temperature and by the addition of radical scavenger. As the effects of temperature and radical scavenger on *E. coli* are different from the strains, it is implied that the amount of some protective substance is different from the strains.

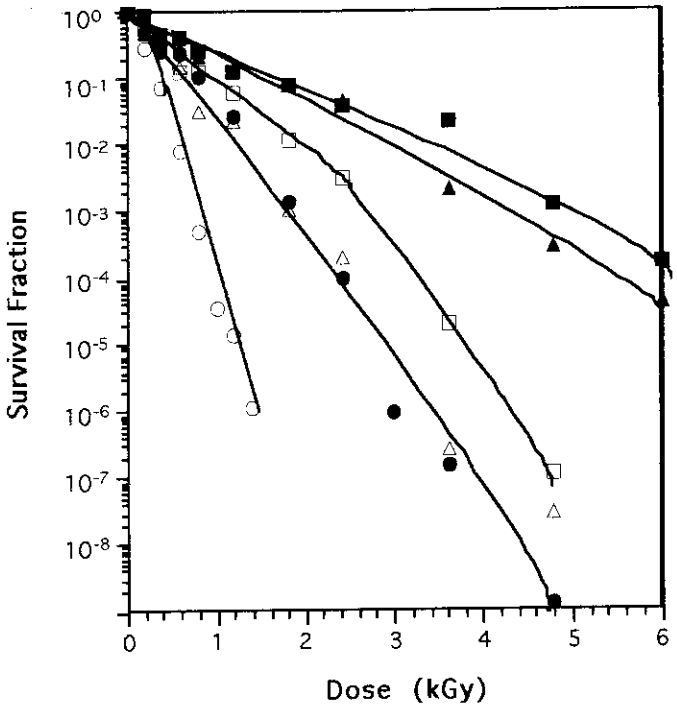

Figure 6 Survival curves of gamma-irradiated *E. coli* B/r. Captions are the same for those in Figures 1 and 3.

Table 1 D_{10} value (kGy) of gamma-irradiated *E. coli*

Strain	*E. coli* B1	*E. coli* B/r
in phosphate buffer solution		
RT	0.13	0.20
Dry-ice-methanol	0.45	0.45
Liquid nitrogen	0.70	0.50
in 5% glycerol solution		
RT	0.45	0.45
Dry-ice-methanol	0.56	1.20
Liquid nitrogen	0.75	1.65

12. Heavy Water and Life Science

Jun Udagawa, Toshihisa Hatta, Hiroshi Omori* and Hiroki Otani
Department of Anatomy and First Department of Surgery*, Shimane Medical University, Izumo 693, Japan

INTRODUCTION

Heavy water (D_2O) has various biological effects. It changes enzyme activities[1], inhibits growth of cells[2] or bacteria[3] and causes malformation[4] in the mouse embryo. In addition to its isotope effect, its solvent effect is important and D_2O has many targets in the biological system. D_2O is effective in various regions and in many steps, therefore, D_2O has complicated effects especially on animals that have rich water. We discuss biological effects of D_2O introducing some results from our experiments.

ABSORPTION AND TOXICITY

D_2O is readily absorbed from gastrointestinal tract as H_2O. Katz et al.[5] reported the course of body fluid deuteration in mice drinking D_2O of various concentrations. After approximately one week, D_2O equilibrates with the body fluid at the level of approximately 80% of the concentration of D_2O in drinking water. Heavy deuteration shortens the life span of mice and mice die when D_2O is substituted for 30 to 40% of the body fluid.

EFFECTS ON GROWTH AND DEVELOPMENT

It has been thought that D_2O inhibits mitosis because it inhibits depolymerization in the mitotic spindle. Lamprecht et al.[6] reported that D_2O affected the conversion of the cytoplasmic microtubule complex into the mitotic spindle, caused a retardation of the prophase/prometaphase transition and blocked metaphase/anaphase transition. They supposed that the antimitotic action of D_2O was attributed to impairment of microtubule-organizing centers. By these or other mechanisms D_2O blocks cell cycle in M phase. It inhibits the division of cultured cells and sea urchin eggs but the effect is instantaneous and reversible. This

suggests that it is important to substitute deuterium for freely-exchangeable hydrogen of the various molecules containing hydrogen of water about this antimitotic effect.

D_2O also delays growth of tumor implanted into nude mice and causes malformation in mouse embryos.

Altermatt et al.[7] reported that growth of human colon carcinoma transplanted into nude mice was inhibited by 30% D_2O administration as drinking water. D_2O especially inhibits the poorly differentiated carcinoma. This effect may be related to proliferation rate of tumor.

Cell division is active and induction of many genes and enzymes occurs in embryos. D_2O can affect the development and cause malformation[4]. We administered 50% D_2O to pregnant female mice and observed embryos at day 11 of gestation. Embryos from deuterated mice were generally smaller than those from non-deuterated mice and 59% of living embryos had defects in the neural tube. Furthermore, large cyst of the head was observed in 8.2% of those embryos.

These effects may be largely due to the antimitotic action of D_2O. However, since D_2O changes various enzyme activities and cell locomotion as in the following section, the effects as above may be related to multiple other actions of D_2O.

EFFECTS ON BIOMOLECULES

There are many enzymes of which activities decrease in D_2O, such as choline acetyltransferase[8], whereas in vivo there are also enzymes of which activities increase in deuterated animals. For example, Thomson and Klipfel[9] reported that the activity of rat liver tryptophan pyrrolase was a little higher in deuterated rats than in non-deuterated rats. Furthermore, they reported that increase in tryptophan pyrrolase activity was considerably less in deuterated rats than in ordinary rats after intraperitoneal injection of tryptophan.

Malaisse et al.[10] reported that D_2O inhibited glucose-induced insulin secretion in tissue culture of pancreatic islets in a dose-dependent manner. They supposed that this effect of D_2O was related to impairment of the microtubular-microfilamentous system that act in the intracellular protein transport.

However, we reported that in the AtT-20 cells, mouse pituitary tumor cells,

cultured in deuterated medium, spontaneous adrenocorticotropic hormone (ACTH) secretion, quantity of intracellular ACTH and proopiomelancortin (POMC; precursor of ACTH) mRNA expression did not decrease[11].

D_2O also affects cell locomotion of fibroblasts. Omori et al.[12] reported that the activities and complexity of cell locomotion decreased and cytoplasmic F-actin increased in D_2O medium. Rate of actin polymerization was accelerated in D_2O although total amount of polymerized action did not change. Although the relation between polymerization rate of actin and alteration of cell locomotion remains unclear, they proved the physical effect of D_2O on polymerization of actin that is one of the cytoskeletal elements. Physical character of D_2O as solvent might be related to the assembly of actin monomers.

EFFECTS ON RHYTHM IN ANIMALS

D_2O administration to the deer mouse, Peromyscus, prolonged its circadian rhythm but this change in rhythm recovered after D_2O administration was stopped[13].

We found prolongation of the hair cycle of nude mice by administration of 30% D_2O and increase in hair length of them at the same time[14]. These phenomena were reversible upon substitution of H_2O for D_2O. These results suggest that D_2O may affect some biological rhythm by unknown mechanisms.

CONCLUSION

Thus D_2O has complicated effects on cells and animals because D_2O acts in multistep and by various manners. Living organisms have much water and water surrounds biomolecules and biomolecules have many hydrogens. The physical character of D_2O is different from that of H_2O, substitution of deuterium for hydrogen in hydrogen bond strengthens this bond and C-D bond is stronger than C-H bond. It is important to consider biological reactions in relation to physical characters of deuterium and this may be key to investigate of role of water and various biomolecules. Furthermore, we could find new biological active products with deuterium that are very useful in medicine.

REFERENCES

1) J. F. Thomson, Biological effects of deuterium., Mac-millan, New York, N.Y. pp.1-133(1963)
2) A. Fischer, Protoplasma, 21, 51(1936)
3) W. Lester, Jr., S. H. Sung and A. Seber, Ann. N.Y. Acad. Sci., 84, 667
4) 田中　修，宇田川　潤，八田　稔久，化学と工業，47(3), 224(1994)
5) J. J. Katz, H. L. Crespi, D. M. Czajka and A. J. Finkel, Am. J. Physiol., 203, 907(1962)
6) J. Lamprecht, D. Schroeter and N. Paweletz, J. Cell Sci., 98, 463(1991)
7) H. J. Altermatt, Jan-Olaf Gebbers and J. A. Laissue, Cancer, 62, 462(1988)
8) S. F. Currier and H. G. Mautner, Proc. Natl. Acad. Sci. USA, 71, 3355(1974)
9) J. F. Thomson and F. J. Klipfel, Biochem. Pharmacol., 3, 283(1960)
10) W. J. Malaisse, F. Malaisse-lagae, M. O. Walker and P. E. Lacy, Diabetes, 20(5), 257(1971)
11) J. Udagawa, T. Hatta, H. Otani and O.Tanaka, J. Deuterium Sci., 4(1), 24(1994)
12) H. Omori, M. Kuroda, H. Naora, H. Takeda, Y. Nio, H. Otani and K. Tamura, Eur. J. Cell Biol., to be submitted.
13) R. B. Suter and K. S. Rawson, Science, 160, 1011(1968)
14) J. Udagawa, T. Hatta, H. Naora, R. Hashimoto and H. Otani, J. Deuterium Sci., 5(2), 15(1996)

Author Index